

Table of contents

List of abbreviations	III
Acknowledgements	V
Abstract	VII
Samenvatting	IX
1 Introduction	11
1.1 Epidemiology	11
1.2 Management of SCI patients	11
1.3 Neuroinflammation in the spinal cord	12
1.4 Role of humoral immune response in SCI	13
1.5 Biomarkers in SCI	14
1.6 Study approach	16
2 Materials and methods	17
2.1 Construction of a hSC cDNA phage display library	17
2.1.1 Poly A+ RNA isolation	17
2.1.2 Conversion of hSC poly A+ RNA into cDNA inserts	17
2.1.3 Cloning of hSC inserts into phage display vectors	19
2.1.4 Characterization of the hSC cDNA libraries	19
2.1.5 Subcloning of the primary hSC cDNA library into pSPVIA and B	20
2.2 Construction of phage display libraries	21
2.3 Plasma samples	21
2.3.1 Preadsorption of plasma samples	21
2.4 Serological antigen selection	22
3 Results	25
3.1 Construction of a primary hSC library	25
3.2 Characterization and identification of the hSC libraries in a pSPVI vector system	27
3.3 Screening of hSC cDNA libraries	29
4 Discussion	31
5 References	35
6 Supplementary	37

List of abbreviations

2x YTAG medium	2x yeast tryptone medium supplemented with ampicillin and glucose
2x YTAK medium	2x yeast tryptone medium supplemented with ampicillin and kanamycin
3' UTR	3' untranslated region
ASIA	American Spinal Injury Association
BLAST	Basic Local Alignment Search Tool
bp	Base pairs
C	Cervical level
cfu	Colony forming units
CNS	Central nervous system
CSF	Cerebrospinal fluid
CT	Computed tomography
DTT	Dithiothreitol
<i>E. coli</i>	<i>Escherichia coli</i>
EDTA	Ethylenediamine-tetraacetic acid
ELISA	Enzyme-linked immunosorbent assay
GFAP	Glial fibrillary acidic protein
h	Hour
hSC	Human spinal cord
Ig	Immunoglobulin
IL	Interleukin
IL-1RA	IL-1 receptor antagonist
kb	Kilobases
min	Minutes
ml	Milliliter
MPBS	Marvel-PBS
MRI	Magnetic resonance imaging
MTBS	Marvel-TBS
NFH	Neurofilament heavy chain
NFL	Neurofilament light chain
PBS	Phosphate buffered saline
PCR	Polymerase chain reaction
pfu	Plaque forming units
rpm	Rounds per minute
RT	Room temperature
s	Seconds
S100b	S100 calcium binding protein b
SAS	Serological antigen selection
SCI	Spinal cord injury
T	Thoracal level
T0	Time point 0 (at admission)
T1	Time point 1 (3 weeks after SCI)
TBS	Tris buffered saline
TNF	Tumor necrosis factor
tSCI	Traumatic spinal cord injury
UniProt	Universal Protein Resource
WT	Wild type

Acknowledgements

During the past eight months, I performed my internship in the immunology – biochemistry group at the biomedical research institute (BIOMED) of Hasselt University. Writing this thesis and the practical training would not be possible without the help of several people, therefore I would like to thank the people who have guided and supported me during this period.

First of all, I would like to thank my promoter Prof. dr. Veerle Somers for the opportunity to perform my senior internship in her research group. I want to thank her for her advice and support, which helped me to perform independent and confident research.

Also thanks to Ilse Palmers for her skilled guidance and critical view on my thesis writing, which has taught me a lot. Thank you for always leaving your door open so I could overload you with all my questions and problems, for the support and helpful advice. Our brainstorming, together with the endless expertise of Igna Rutten, about problems that pop-uped during the practical internship taught me how to think beyond the scope and solve these points at issue. Furthermore, thanks to the immunology – biochemistry group and especially dr. Wendy Hansen and dr. Steven Haesendonckx for critically evaluating my senior thesis. Moreover, a word of appreciation to my second examiner dr. Patrick Vandormael for his critical evaluation of my senior project and his problem solving skills.

Finally, I would like to thank my fellow students, for letting me pour my heart out at difficult moments and for helping me with their expertise. We had some great unforgettable times in the student room. A special thanks to my parents for giving me the opportunity to study and also for their support during the last five years.

Abstract

Spinal cord injury (SCI) is a devastating condition caused by a trauma to the spinal cord. A reliable biomarker is required to estimate the severity of the lesion, which will improve the diagnosis, prognosis and theranosis in SCI. Biomarker research will also provide more insights into the antibody response present after SCI.

SCI is characterized by two phases of damage, the primary (caused by the original trauma) and secondary damage. One of the major contributors of secondary damage is neuroinflammation, which affects the neighboring healthy tissue and expands the initial lesion. Animal and human studies showed that pathogenic antibody levels were elevated after SCI. Still, the exact role of these antibodies and their targets are unknown in humans.

Since SCI-induced antibodies play a pivotal role during the neuroinflammation, the goal of this study is to identify novel candidate antibody biomarkers relevant in human SCI pathology by using serological antigen selection (SAS). SAS is a high-throughput technique that uses phage display to identify pathologically relevant antibodies and their targets. In the present study, human spinal cord (hSC) cDNA libraries were constructed, which were analyzed for their relevance by titration, polymerase chain reaction (PCR) and sequencing. Subsequently, hSC cDNA libraries were cloned into three pSPVI phage display vectors and expressed on the surface of filamentous phage. Phage displaying the cDNA library were screened for antibody reactivity by using pooled plasma from traumatic SCI (tSCI) patients. After four rounds of selection not enough enrichment of specific clones was observed. A fifth selection round has to be performed with modified selection conditions.

Samenvatting

Ruggenmergschade is een ernstige conditie die veroorzaakt wordt door een trauma aan het ruggenmerg. Betrouwbare biomerkers zijn vereist voor de ernst van de laesie in te schatten, deze zullen de diagnose, prognose en therapie verbeteren in ruggenmergschade. Het onderzoek naar biomerkers zal ook meer informatie geven over de aanwezige antilichaam respons na een ruggenmergschade.

Ruggenmergschade wordt gekarakteriseerd door twee fasen van schade, de primaire (veroorzaakt door de initiële trauma) en secundaire schade. Neuroinflammatie speelt een belangrijke rol tijdens de secundaire schade, die het aangrenzend gezond weefsel aantast en de initiële laesie verder uitbreidt. Dierstudies en humane studies tonen aan dat verhoogde concentraties van pathogene antilichamen aanwezig zijn na ruggenmergschade. Nochtans is de exacte rol van deze antilichamen en hun antigenen in de mens nog niet gekend. Daarom is doel van deze studie de identificatie van nieuwe kandidaat antilichaam biomarkers die relevant zijn in humane ruggenmergschade pathologie door gebruik te maken van serologische antigeen selectie (SAS).

SAS is een techniek die gebruik maakt van een faag expressiesysteem om zo pathologisch relevante antilichamen en hun antigenen te identificeren. In de huidige studie werd er een humane ruggenmerg cDNA bank ontwikkeld die geanalyseerd werd voor zijn relevantie door middel van titraties, polymerasekettingreacties en sequentie bepalingen. Vervolgens werd de humane ruggenmerg cDNA bank gekloneerd in drie pSPVI faag expressievectoren. De overgekloneerde cDNA banken werden tot expressie gebracht op het oppervlak van filamenteuze fagen. Fagen die de cDNA bank tot expressie brengen worden gescreend voor antilichaam reactiviteit door gebruik te maken van gepoold plasma van traumatische ruggenmergschade patiënten. Na vier selectie rondes was er onvoldoende aanrijking aanwezig van specifieke klonen, hierdoor moet een vijfde ronde uitgevoerd worden met aangepaste selectie condities.

1 Introduction

1.1 Epidemiology

Spinal cord injury (SCI) is defined as any trauma to the spinal cord, which is not caused by a disease. Trauma to the spinal cord is most often caused by motor vehicle accidents, acts of violence, falls and injuries from recreational activities (1, 2). Traumatic SCI (tSCI) affects mainly young males between the age of 18 and 30 years, but also elderly in the age group of 55 - 74 due to ground-level falls (2, 3). The worldwide annual incidence of tSCI is 12.1 – 57.8 cases per million people (4) and the prevalence is reported to be between 236 - 4187 patients per million people (5). In Europe, the incidence of tSCI is estimated to vary between 3.3 and 130.6 individuals per million inhabitants (6). The prevalence in Western Europe is 280 – 316 patients per million people (5). SCI is a devastating condition, which not only affects the patient but also the society. SCI patients have an impact on the health care system in the acute phase of the disease as well as in subsequent years due to secondary complications (e.g. urinary tract infections, pneumonia), long-term care admissions, home care services, physician contacts and other common health care problems (e.g. psychological conditions) (7, 8). Because of improved care of SCI patients, a continuous increase in the life expectancy is observed. SCI patients that have been affected between the age of 25 and 34 years have a median survival of 38 years post-injury, with a surviving chance of 43% for at least 40 years (7).

1.2 Management of SCI patients

Currently, the diagnosis of SCI is based on neurological symptoms and imaging procedures. Initially, a neurological examination is performed during which the mental status, autonomic functions, motor function and sensation are evaluated. The American Spinal Injury Association (ASIA) classification is standardly used to describe and classify the severity of a SCI based on the degree of sensory and motor impairment (1, 2). The classification ranges from A to E with A corresponding to a complete injury (no sensory or motor functions are preserved in sacral segments 4-5), B represent an incomplete injury (partial preservation of sensory functions below the neurological level and sacral segments S4-5), C and D are incomplete injuries (preservation of motor functions below the neurological level and a muscle grade of less (C) or more (D) than three in half of the key muscles below the neurological level) and class E (sensory and motor functions are normal). A major limitation in the ASIA classification is that it is only reliable when conducted 72 hours post-trauma (4, 9).

Most frequently used imaging procedures to diagnose SCI are computed tomography (CT) and magnetic resonance imaging (MRI). CT is preferred as imaging tool to assess the anatomy of spinal bones in SCI patients, while MRI is the method of choice to evaluate the damage to the spinal cord (4, 10). These imaging procedures, however, also have their limitations. For example, SCI patients with multiple injuries are too unstable for MRI. A second limitation is that MRI only shows the macroscopic changes in the spinal cord, while the visualisation of the microscopic injury is lacking. Another limitation is that the white matter imaging is rather limited, while the remaining functions

after SCI are mainly determined by the degree and localization of the damaged/spared white matter (4, 10-12).

Age and adjunctive physiological testing are nowadays used to estimate the clinical outcome, but have a limited prognostic value (1, 13). Several sources claim that there is no difference in neuronal recovery potential following SCI between elder and younger individuals (14, 15), which implies that age has a low prognostic value. However, from a clinical point of view a difference has been observed between elderly and youngsters in neuronal recovery (16). In addition, an increasing age is also a risk factor for complications (e.g. urinary tract infections, pressure sores, etc.) (17). Furthermore, not all SCI patients can contribute to physiological examinations due to cognitive impairment, which indicates that the physiological status cannot be assessed for every patient (13). Due to limitations in neurological examination, imaging procedures and estimation of the clinical outcome, novel biomarkers are needed that can contribute to the diagnosis and prognosis of SCI.

Treatment options of SCI are limited and dependent on the injury itself. A surgical intervention may be needed to decompress and stabilize the swollen spinal cord by removing the damaged bones, CSF accumulations and disc and ligament fragments. Medication is used for pain management and the prevention of complications (e.g. urinary tract infections, deep vein thrombosis, etc.). An example of such medication is methylprednisolone, which is a steroid drug. Methylprednisolone is investigated for its neuroprotective effect, however a lot of controversy exists about the use of this drug in SCI (18-22). Revalidation is also a major part of the treatment and focusses on the improvement of existing functions, rehabilitation and reintegration of SCI patients into society (1). Nowadays, a lot of clinical trials are ongoing to find new therapies for spinal cord injury patients. SCI patients with a severe lesion react differently to neuroprotective therapies compared to patients with a less severe lesion (12). A solution for this is a biomarker that could contribute in the clinic to distinguish between SCI severities and assign the appropriate neuroprotective treatment for a particular SCI patient.

1.3 Neuroinflammation in the spinal cord

Two phases of damage can be distinguished after SCI. The primary damage is caused by mechanical trauma and leads to compression, contusion, transection or laceration of the spinal cord. The initial lesion results in loss of sensory, motor and/or autonomic functions. The secondary damage involves a chain of interrelated reactions, which are initiated by the primary damage and involves oedema, disruption of the vasculature, permeability of the blood-spinal cord barrier, ionic toxicity, cell death (apoptosis and necrosis), excitotoxicity, demyelination, axonal degeneration and inflammation. Neuroinflammation in the spinal cord is one of the major contributors to secondary damage. Components of this reaction are macrophages, neutrophils and microglia that produce products containing pro-inflammatory cytokines, reactive oxygen species and matrix metalloproteinases, which exacerbate inflammation. The interrelated reactions affect the surrounding healthy tissue and cause an expansion of the initial lesion. Secondary damage results in the substantial loss of oligodendrocytes and neurons, glial scar formation and cavitation which limit functional recovery. Despite causing further damage, the neuroinflammatory reaction is also necessary to induce recovery of the lesion (e.g. by clearance of cellular debris) (1, 23-25).

1.4 Role of humoral immune response in SCI

SCI is associated with damage to the blood-spinal cord barrier and cell death. Central nervous system (CNS) antigens derived from injured tissue come into the circulation (Figure 1 [1]), which trigger the immune system. Subsequently, antigen presenting cells activate T cells (Figure 1 [3]). Animal studies show that CNS-reactive T cells are activated and aggravate neuropathology after SCI (26, 27). Activated T cells are able to interact with B cells resulting in cell proliferation, differentiation and antibody production (Figure 1 [2]) (28, 29). Indeed, activation of B cells after SCI is observed in mice by a marked increase in the number of B cells and the production of pathogenic antibodies (30). Circulating B cells and immunoglobulins (Ig) move across the damaged blood-spinal cord barrier and accumulate at the site of injury (28), which is confirmed in SCI mice (29, 30). Furthermore, B cells formed follicle-like structures as a result of the continuous accumulation of B cells and antibodies at the trauma site during the chronic phase of SCI (weeks to months after SCI) (Figure 1) (28). Spontaneous neurological recovery after SCI was improved in B cell knockout mice compared with wild type (WT) mice, which implies that B cells contribute to the inflammatory response after SCI (28, 30). Lucin and colleagues demonstrated that B cells produce pathogenic antibodies after a mid-thoracic SCI (T9-T10) in mice, whereas there was an immune suppression, also towards the B cell function, after a high thoracic SCI (T3-T5) (31). This can be explained by a disrupted regulation of the immune system in high thoracic SCI (23). Additionally, an injection of purified antibodies from SCI mice into healthy spinal cord tissue of WT mice induced persistent paralysis and SCI pathology (30), indicating the degenerative effect of these SCI-induced antibodies.

In humans, it has been shown that elevated CNS autoantibody levels and myelin-reactive antibody levels are present in serum and cerebrospinal fluid (CSF) after SCI (30, 32, 33). Autoantibodies against myelin basic protein and brain gangliosides were raised in sera of tSCI patients (33). Davies and colleagues have shown that the concentration of interleukin (IL) 6, tumor necrosis factor (TNF)- α , IL-1 receptor antagonist (IL-1RA) and GM1 ganglioside IgG was higher in individuals with SCI compared to healthy volunteers. Serum levels of proinflammatory cytokines and autoantibodies are more elevated in SCI patients with secondary complications (neuropathic pain, urinary tract infections and pressure ulcers) compared to patients without secondary complications. This finding may indicate that a protective autoimmune response is present as a consequence of a latent or explicit infection or an immune-mediated axonal conduction deficit caused by cytokine dysregulation. (34). Human studies showed that antibodies are elevated after a SCI. From animal studies we know that these antibodies have a detrimental effect on the surrounding healthy tissue. Both animal and human findings make these SCI-induced antibodies useful for the examination of disease processes that contribute to post-SCI pathology and to develop a biomarker that evaluates SCI.

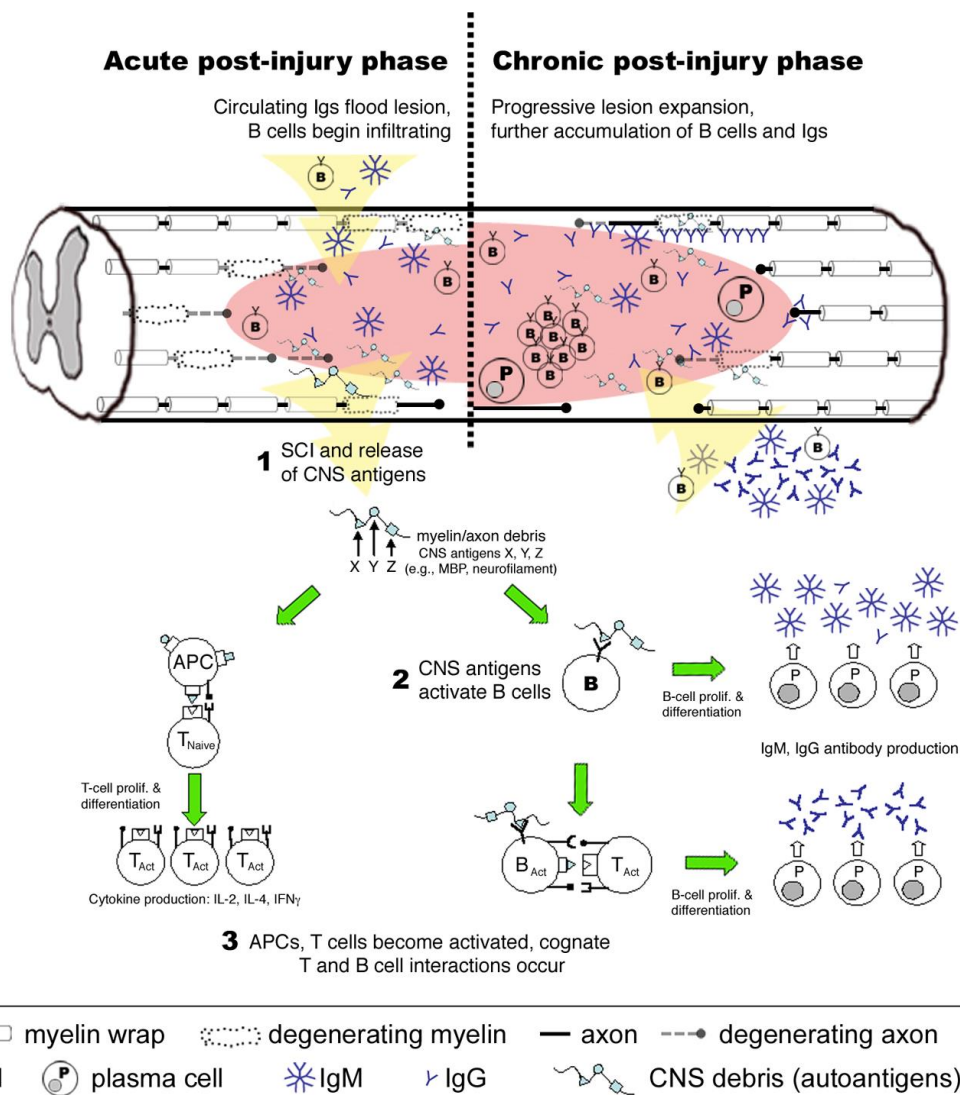


Figure 1: Potential mechanism of B cell activation in tSCI (28). Damage to the spinal cord disrupts the blood-spinal cord barrier. Central nervous system (CNS) antigens are released in the circulation and activate the immune system. T cells become activated due to CNS antigen presentation by antigen presenting cells (APCs) [3]. B cells get activated by interaction with T cells and recognition of CNS antigens, which leads to proliferation, differentiation and antibody production [2]. B cells and antibodies infiltrate into the spinal cord [1]. In the chronic phase, follicle-like structures form as a result of the continuous accumulation of B cells at the trauma site.

1.5 Biomarkers in SCI

A biomarker is a parameter, which is objectively measured and assessed as a marker of normal or pathological processes (4). An ideal biomarker needs to have an early and significant release into blood or CSF after an injury, and must be specific for the CNS. Furthermore, the biomarker is only useful when there is a relationship between the concentration of the marker and the parameter to be evaluated (e.g. injury severity, therapy effectiveness, etc.). Other important properties are a minimal influence of confounding factors, reproducibility of the outcome and inexpensiveness (35). Attempts have already been undertaken to find biomarkers for SCI, mostly in animal models (Table 1) (11).

Table 1: Potential SCI biomarkers and their attributes (11).

Candidate marker	Molecule	Marker origin	Attributes
S100b	Protein	Glia	CNS injury marker
GFAP	Protein	Glia	Gliosis/glia cell injury
MBP	Protein	Oligodendrocytes/ Schwann cells	Demyelination
SBDP150/SBDP145	Protein	Axon (calpain-generated)	Acute necrosis
SBDP120	Protein	Axon (caspase-3-generated)	Delayed apoptosis
UCH-L1	Enzyme	Neuronal cell body	Neuronal cell body injury
MAP2	Protein	Dendrites	Dendritic injury
Neurofilament proteins: NFL, NFM, NFH	Protein	Cytoskeletal component	Axonal injury markers
NSE	Enzyme	Cytoplasm of neurons	Neural damage marker
IL-1 β , TNF- α , IL-6, and other cytokines	Cytokine	Microglia/infiltrating macrophage	Neuroinflammation

CNS: central nervous system, S100b: S100 calcium binding protein b, GFAP: glial fibrillary acidic protein, IL: interleukin, MAP2: microtubule-associated protein 2, MBP: myelin basic protein, SBDP: spectrin breakdown product, TNF: tumor necrosis factor, UCH-L1: ubiquitin C-terminal hydrolase-L1, NFL: neurofilament light chain, NFM: neurofilament medium chain, NFH: neurofilament heavy chain, NSE: neuron-specific enolase

Biomarker discovery has also been undertaken in humans. Guez and colleagues were the first to show an increased concentration of neurofilament light chain (NFL) and glial fibrillary acidic protein (GFAP) in CSF of six tSCI patients compared to neurological healthy controls (n=24). NFL is a protein involved in the structuration of neurons and is mainly localized in axons. GFAP is a filament protein that is generally located in astroglial cells. Both NFL and GFAP levels can give an indication of the amount of nerve cell damage (36). However, no major conclusions can be drawn from this paper due to several research limitations. In this study only six SCI patients were included and time of sampling varied (1-21 days). Furthermore, no correlation was made between the concentration of the marker and the neurologic deficit or functional recovery and no statistical analysis was performed on the obtained data (12). Kwon and colleagues performed a larger prospective study in which they gathered CSF samples between the time of injury and 72 hours post-injury of 27 SCI patients with complete (ASIA A) or incomplete (ASIA B/C) SCI. Cytokine and protein concentrations were measured and compared between three injury degrees (ASIA A, B and C). CSF concentrations of S100 calcium binding protein b (S100b), GFAP and IL-8 were able to predict the injury degree in 89% of the patients. These putative biomarkers were able to determine the motor outcome at six months better compared to the standard ASIA classification (37). Hayakawa and colleagues collected plasma instead of CSF samples (6h – 21 days post-injury) from 14 acute cervical SCI patients and determined the neurofilament heavy chain (NFH) concentration. Plasma NFH concentrations were compared among different ASIA grades. A significant difference in NFH concentration was observed between complete (ASIA A) and incomplete (ASIA C) SCI patients, showing that NFH could serve as a potential biomarker for determining the severity of the SCI (38). Pouw and colleagues identified differences in CSF concentrations of NSE, S-100b and NFH between motor complete and incomplete

tSCI patients (39). Their findings highlight several potential biomarkers for which further validation is warranted.

1.6 Study approach

The goal of this study is to identify novel candidate antibody biomarkers to provide more insight into the antibody response present after SCI. We hypothesize that serological antigen selection (SAS) will lead to a panel of candidate antibody biomarkers relevant in SCI pathology since it has been successfully applied specifically for this end in multiple sclerosis (40), rheumatoid arthritis (41), clinical isolated syndrome (42), etc.

SAS is a technique that uses phage display to identify pathologically relevant antibodies and their targets (43). A human spinal cord (hSC) cDNA library will be cloned into a phage display vector system (pSPVI) and packaged in filamentous phage using M13K07 helper phage. Subsequently, the resulting displayed proteins will be screened for antibody reactivity using pooled plasma samples of tSCI patients (Figure 2). Antigen-antibody complexes will be captured and phage are enriched by exposing them to several selection rounds using the same plasma pool (44). Finally, proteins that are expressed on the surface of enriched phage will be analysed by using polymerase chain reaction (PCR), restriction digestion and sequencing.

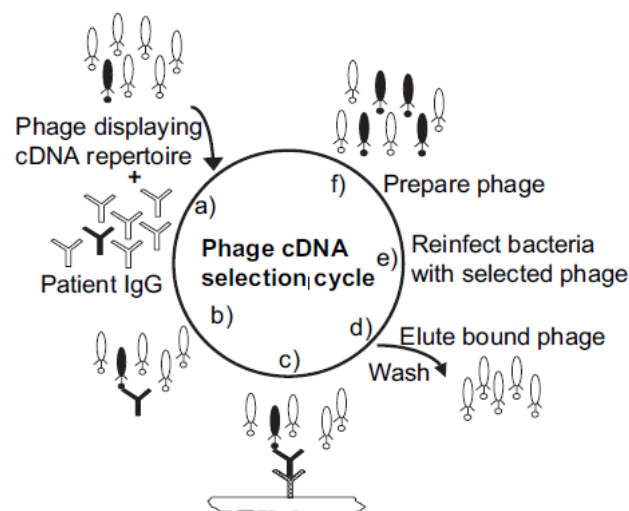


Figure 2: SAS procedure (43). First, phage displaying the normal spinal cord cDNA library will be incubated with pooled patient's plasma (a), so that antibody-antigen complexes are formed (b). Antibody-antigen complexes are captured on a surface coated with rabbit anti-human IgG enriching for antigens specifically recognized by plasma IgG antibodies (c). Unbound phage will be washed away and antibody-antigen complexes will be eluted (d). Eluted phage will be amplified by reinfection in *E. coli* TG1 cells (e). These amplified phage will be used as input for the following selection round (f).

2 Materials and methods

2.1 Construction of a hSC cDNA phage display library

A hSC cDNA phage display library was constructed into three phage expression vectors to perform the SAS procedure (Figure 3).

2.1.1 Poly A+ RNA isolation

The hSC cDNA library was constructed by using commercially obtained hSC poly A+ RNA derived from normal spinal cords of 18 Caucasians (25 - 63 years) who died suddenly. Obtained poly A+ RNA was purified by two selection rounds on oligo(dT)-cellulose columns after being isolated with a modified guanidinium thiocyanate method (Clontech, California, USA).

2.1.2 Conversion of hSC poly A+ RNA into cDNA inserts

5 µg hSC poly A+ RNA was converted to double stranded cDNA (Figure 3a) by using the SuperScript Choice System for cDNA Synthesis (Invitrogen, Paisley, UK), according to manufacturer's instructions with minor modifications. In the first strand synthesis, 3 µg oligo(dT) primer with XhoI linker (GAGAGAGAGAGAGAGAGAGAACTAGTCTCGAGTTTTTTTTTTTTTTTTTTT, Eurogentec, Seraing, Belgium) together with 5 µg hSC poly A+ RNA was heated for 10 minutes (min) at 70°C and quick-chilled on ice to obtain linear mRNA. The first strand synthesis mixture was supplemented with 0.02 M dithiothreitol (DTT), 1x First Strand Buffer, dNTP mix (100 mM dATP, dGTP and dTTP and 10 mM methylated dCTP) and placed at 37°C for 2 min to inactivate potential RNases. Methylated dCTPs were used to prevent restriction of the hSC inserts by restriction enzymes later on in the procedure. SuperScript II Reverse Transcriptase (1000 U) was added to the first strand mixture and incubated for 1 hour (h) at 37°C to obtain cDNA-RNA hybrids. The reaction was terminated by cooling on ice. 1x Second Strand buffer and dNTP mix (10 mM dATP, dGTP and dTTP and 26 mM dCTP) were added to the first strand mix, together with *Escherichia coli* (*E. Coli*) RNase H (2 U) for breaking down the RNA template. Subsequently, *E. coli* DNA polymerase I (40 U) was added to the mixture to correctly pair added-nucleotides with the base pairs of the existing cDNA strand. Ligation of adjacent nucleotides was fulfilled during the second strand reaction by *E. coli* DNA ligase (10 U). The second strand mixture was incubated for 2 h at 16°C to obtain double stranded cDNA. cDNA fragments were blunted by using 10 U T4 DNA Polymerase (16°C, 15 min) and the reaction was stopped by addition of 0.5 M ethylenediaminetetraacetic acid (EDTA). A Phenol:chloroform:isoamyl alcohol precipitation was followed by ethanol washes to purify the cDNA. EcoRI adapters (AATTCGCGGCCGCGTTCGAC, Invitrogen, Paisley, UK) were ligated to blunt-ended double stranded cDNA segments using 5 U T4 DNA ligase, adapter buffer, 10 µg EcoRI Adapters and 0.1 M DTT (16°C, 16 h). After heat-inactivation (10 min, 70°C), EcoRI-adapted cDNA was phosphorylated by addition of 30 U T4 Polynucleotide Kinase for 30 min at 37°C, which is inactivated afterwards for 10 min at 70°C. Subsequently, a XhoI overhang was obtained by applying 20 U XhoI (Promega, Madison, USA), 1x restriction enzyme buffer and 0.1 mg/ml acetylated BSA. The digestion was incubated for 3 h at 37°C and was followed by an inactivation at 65°C for 15 min.

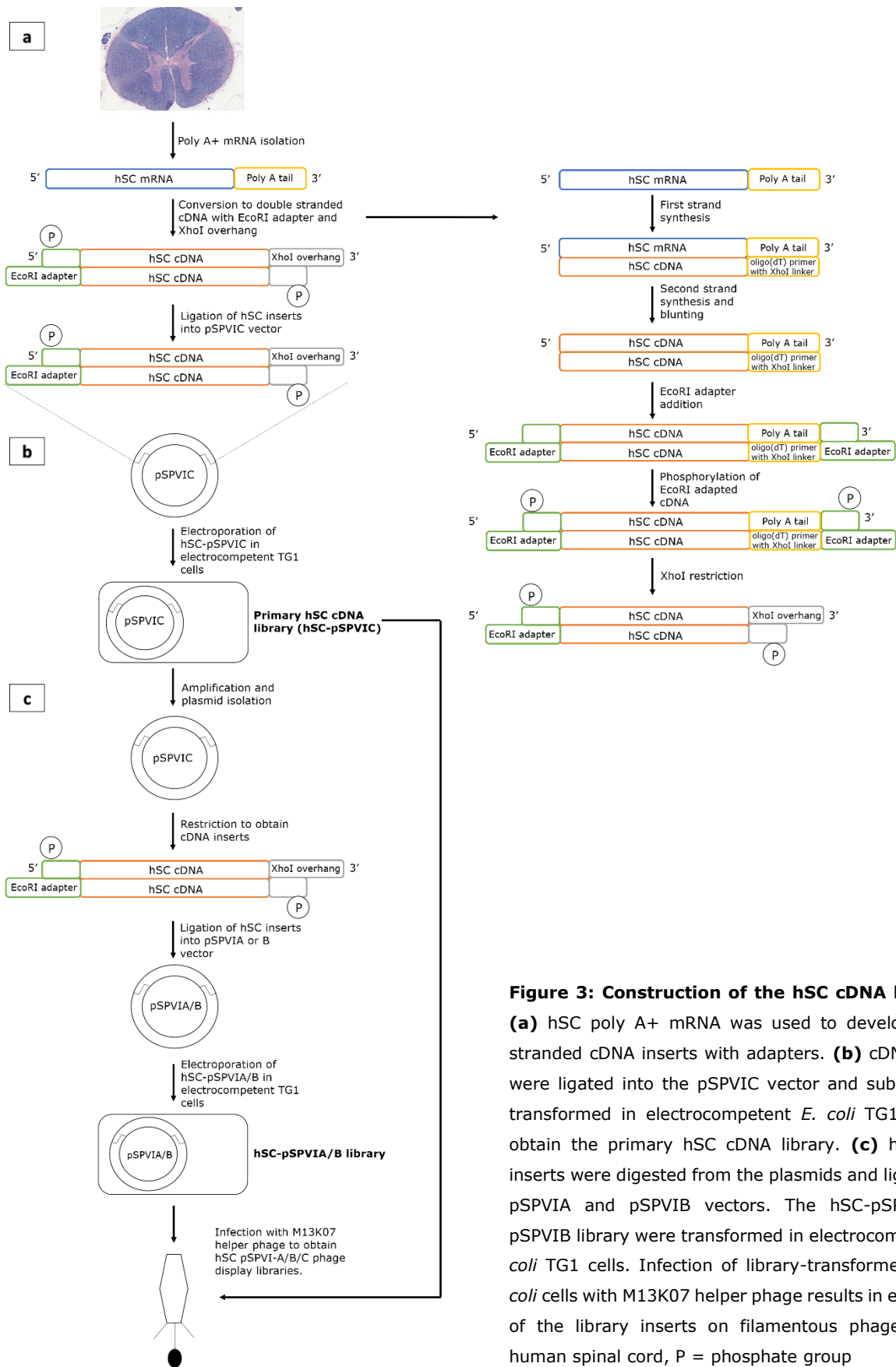


Figure 3: Construction of the hSC cDNA libraries. (a) hSC poly A+ mRNA was used to develop double stranded cDNA inserts with adapters. (b) cDNA inserts were ligated into the pSPVIC vector and subsequently transformed in electrocompetent *E. coli* TG1 cells, to obtain the primary hSC cDNA library. (c) hSC cDNA inserts were digested from the plasmids and ligated into pSPVIA and pSPVIB vectors. The hSC-pSPVIA and pSPVIB library were transformed in electrocompetent *E. coli* TG1 cells. Infection of library-transformed TG1 *E. coli* cells with M13K07 helper phage results in expression of the library inserts on filamentous phage. hSC = human spinal cord, P = phosphate group

50 µl of TEN buffer (10 mM Tris-HCl pH 7.5, 0.1 mM EDTA, 25 mM NaCl, autoclaved) was added to hSC cDNA with adapters and gently mixed. The entire sample was administered to the cDNA size fractionation column and the effluent was collected in the first fraction. A total of 20 fractions were collected by re-applying 100 µl TEN buffer to the column each time. Concentrations of the collected fractions were determined by using the Nanodrop 2000c (Thermo Scientific, Wilmington, USA). Fractions 1-12, 13-16 and 17-20 were pooled and purified using the illustra GFX PCR DNA and Gel Band Purification Kit (GE Healthcare, Buckinghamshire, UK), followed by determination of the concentration and purity. Column chromatography was used to purify and size fractionate cDNA fragments, to enrich for larger inserts and to remove residual adapters.

2.1.3 Cloning of hSC inserts into phage display vectors

3 µg phage display vector pSPVIC (Figure 4) was digested using 10 U EcoRI (New England Biolabs, Massachusetts, USA), 10 U Xho I (Promega, Madison, USA), 1x NEB4 buffer, 0.1 mg/ml acetylated BSA and incubated for 3 h at 37°C. Subsequently, 5 µl orange G (10 mg in 50 ml milli Q and 3% glycerol) was added to the mixture and loaded on a 1% agarose gel stained with 1:10000 ethidium bromide (Merck, Darmstadt, Germany). 100 base pairs (bp) and 1 kilobase (kb) DNA ladders (Invitrogen, California, USA) were also loaded on the agarose gel. Vectors (3500 bp) were purified by using the illustra GFX PCR DNA and Gel Band Purification Kit according to manufacturer's recommendations.

hSC cDNA fragments, containing an EcoRI and XhoI adapter, were ligated in a 1:20 (vector:insert) ratio into the EcoRI/XhoI digested phage display vector pSPVIC using 3U T4 DNA ligase (Promega, Madison, USA) and 1x ligase buffer (Figure 3b). Ligation mixtures were incubated for 18 h at 15°C to obtain the primary hSC-pSPVIC library.

The primary hSC-pSPVIC library was electroporated in electrocompetent *E. coli* TG1 cells ([F' traD36 proAB lacIqZ ΔM15] supE thi-1 Δ(lac-proAB) Δ(mcrB-hsdSM)5(rK⁻mK⁻), Lucigen, Middleton, USA) by using the MicroPulser Electroporator (Bio-Rad, California, USA) (Figure 3b). Electroporations were performed according to the manufacturers' protocol of electrocompetent *E. coli* TG1 cells. Transformed cells were plated (1/100 diluted) on 2xYTAG agar plates (2x yeast-tryptone medium (BD, Le Pont de Claix, France) supplemented with 15 g Bacto Agar (BD, Le Pont de Claix, France), 2% glucose (Merck, Damstadt, Germany) and 100 µg/ml ampicillin (Roche Diagnostics, Vilvoorde, Belgium)) and incubated overnight at 30°C. The number of colonies formed was used to determine the concentration in colony forming units (cfu) per millilitre (ml). Glycerol stocks were made (15% glycerol) by scraping off colonies from the plate and stored at -80°C.

2.1.4 Characterization of the hSC cDNA libraries

The titer, identity and diversity were determined to characterize the hSC cDNA libraries. A dilution series in 2xYT medium containing a hSC cDNA library were plated out on 2xYTAG plates and grown overnight at 30°C to determine the titer. Titer was calculated by: number of colonies x dilution factor x 10.

To determine diversity, colony PCR was performed on individual colonies to evaluate presence and size of the inserts. PCR reaction mix consisted out of 1x PCR reaction buffer, 0.2 mM dNTP, 0.2 μ M pUC reverse primer (CGCCAGGGTTTTCCAGT, eurogentec, Seraing, Belgium), 0.2 μ M gene 6 forward primer (TTACCCTCTGACTTTGTTCA, eurogentec, Seraing, Belgium) and 2 U Taq DNA polymerase (Roche, Mannheim, Germany). One single colony was added to 50 μ l PCR mix. The PCR reaction was subjected to an initial denaturation step for 10 min at 95 °C, followed by 35 cycles (30 seconds (s), 95 °C; 30 s, 55 °C; 2 min, 72 °C) of PCR amplification and a final elongation at 72 °C for 10 min in the iCycler Thermal Cycler (Bio-Rad, California, USA). Amplification products were analysed on a 2% agarose gel stained with 1:10000 ethidium bromide, which was also loaded with 100 bp and 1 kbp DNA ladders. Diversity was determined by calculation of the insert sizes and the percentage of recombination.

cDNA inserts with the same length were checked for a same restriction pattern (fingerprinting) to have indication about insert identity. Fingerprinting was performed using 5 U BstNI (Roche, Mannheim, Germany), 2x SuRE/Cut buffer H (Roche, Mannheim, Germany) and 10 μ l PCR product. Samples were incubated for 2 h at 37°C followed by electrophoresis on a 2% agarose gel stained with 1:10000 ethidium bromide. 100 bp and 1 kb DNA ladders were also loaded on the agarose gel. Digestion patterns from the restricted inserts were determined and compared to each other.

To determine the exact identity, diversity and potential function of the hSC cDNA inserts, sequencing analysis was performed. 2 μ l ExoSAP-IT (GE, Cleveland, USA) was added to 5 μ l PCR product (15 min at 37°C, 15 min 80°C) to remove unconsumed dNTPs and primers. Subsequently, purified PCR samples were used to perform sequencing PCR, which contained 1x Big Dye Buffer (Applied Biosystems, California, USA), sequencing mix (Applied Biosystems, California, USA), 0.2 μ M gene 6 forward primer and 1 μ l purified PCR sample (hot start at 90°C, 30 s at 96 °C, followed by 25 cycles (10 s, 96 °C; 5 s, 50 °C; 4 min, 60 °C)). Next, samples were administered to a Sephadex G50 (GE Healthcare, Diegem, Belgium) column and centrifuged for 2 min at 3200 rounds per minute (rpm). Eluent was evaporated and pellet dissolved in 25 μ l Hi-Di Formamide (Applied Biosystems, California, USA). Samples were loaded on the ABI Prism 310 genetic analyser (Applied Biosystems, California, USA) for sequence analysis. Resulting nucleotide and amino acid sequences were compared to GenBank databases by using the basic local alignment search tool (BLAST, <http://blast.ncbi.nlm.nih.gov/Blast.cgi>).

2.1.5 Subcloning of the primary hSC cDNA library into pSPVIA and B

100 times the diversity of the primary hSC cDNA library was grown in 2xYTAG medium (37°C, 180 rpm, 8 h). The culture was diluted 1:125 in 2xYTAG medium and grown overnight at 37°C, 180 rpm. Plasmid isolation was performed on the overnight culture by using the Qiagen Plasmid Midi Kit (Qiagen, Venlo, The Netherlands), according to manufacturers' instructions. A restriction digestion with 20 U XhoI, 20 U EcoRI, 1x NEB4 buffer, 0.1 mg/ml acetylated BSA was performed on 10 μ g hSC-pSPVIC plasmid (see section 2.1.3). EcoRI and XhoI restricted hSC cDNA inserts were ligated in a 1:20 (vector:insert) ratio in EcoRI/XhoI digested pSPVIA and B (see section 2.1.3). Subsequently, ligation mixtures were electroporated in electrocompetent *E. coli* TG1 cells (see

section 2.1.3), to obtain hSC-pSPVI A and B libraries (Figure 3c). Both libraries were characterized as described before (2.1.4).

2.2 Construction of phage display libraries

To express the hSC cDNA libraries on the surface of filamentous phage, bacterial glycerolstock (100 times the diversity) of the three hSC-pSPVI libraries was infected with M13K07 helper phage (Amersham Biosciences, New Jersey, USA) (Figure 3c), in a ratio phage:bacteria between 10:1 and 20:1. The infection mixture was incubated for 30 min at 37°C followed by centrifugation for 10 min at 4000 rpm. Supernatant was removed and the bacterial pellet was resuspended in 25 ml 2xYTAK (2x yeast-tryptone medium supplemented with 100 µg/ml ampicillin and 50 µg/ml kanamycin (Life Technologies, California, USA)) medium. Infected bacteria were grown overnight at 30°C and 180 rpm. The bacterial suspension was centrifuged at 4000 rpm for 20 min (4°C). Supernatants was precipitated with 1:5 volume 20% PEG/NaCl for 1 h on ice and centrifuged for 15 min at 4000 rpm (4°C). Phosphate buffered saline (PBS) wash steps followed by centrifugation (5 min, 14000 rpm, 4°C) were repeated until a white pellet was present in order to remove contaminating bacteria. The phage pellet was resuspended in 1 ml PBS and centrifuged for 2 min at 14000 rpm. Supernatant with the phage was stored at 4°C until use.

2.3 Plasma samples

Plasma samples of 10 SCI patients were used to perform the SAS procedure. Blood from SCI patients was obtained at admission to the hospital and 3 weeks post-trauma (Table 2). Plasma was isolated by centrifugation at 2000 rpm for 10 min and a second time at 3900 rpm for 10 min to remove remaining red blood cells. Plasma was aliquoted and stored at -80°C.

2.3.1 Preadsorption of plasma samples

To remove antibodies specific for phage and *E. coli* extracts, plasma samples were preabsorbed. *E. coli* extracts (Y1090, Promega, Madison, USA) were commercially obtained. Phage extracts were made by using M13K07 helper phage. *E. coli* TG1 bacteria (OD₆₀₀=0.7, 50 µl of stock) were added to serial dilutions (10⁻³, 10⁻⁴ and 10⁻⁵ cfu/ml) of helper phage M13K07, and incubated for 30 min at 37°C. *E. coli* TG1 bacteria (OD₆₀₀=0.7) were extra added to the infected dilutions and plated on 2xYT agar plates in solution with 2xTY top agar (overnight incubation at 30°C).

An individual plaque was pricked and resuspended in 2xYT medium with 1:100 overnight *E. coli* TG1 culture and incubated for 2 h at 37°C and 180 rpm to allow infection. 150 ml 2xYT was added and the mixture was incubated for 1 h at 37°C and 180 rpm allowing expression of the kanamycin resistance gene. Next, 50 µg/ml kanamycin was added and cultures were grown overnight (37°C, 180 rpm). The overnight culture of M13K07 helper phage was centrifuged for 20 min at 2800 g (4°C). Phage were precipitated as described before (2.2). Phage pellets were resuspended in 5 ml PBS and completely destroyed by sonification (three times for 10 s on ice). Phage or *E. coli* extracts were coupled to 1 gram of Cyanogen bromide-activated–Sepharose 6MB (Sigma-Aldrich, St. Louis, USA), according to manufacturers' protocol. The mechanical (*E. coli*) and lytic (M13K07 helper

phage) columns were centrifuged for 3 min at 1500 rpm and supernatant was removed. 3-4 ml beads from each column were washed two times in 10 ml TBS (tris buffered saline, 20 mM Tris-HCl pH 7.5 and 150 mM NaCl) for 5 min. After centrifugation (3 min, 1500 rpm), the supernatant was removed. 200 µl of each plasma sample (Table 2), 8 ml 0.1% marvel-TBS (MTBS) and 100 µl 5% sodium azide solution were added to the mechanical column and incubated overnight at 4°C on an end-over-end rotor. The supernatant of the mechanical column was transferred to the lytic column and incubated overnight at 4°C on an end-over-end rotor. Subsequently, the column was centrifuged for 5 min at 2000 rpm and the supernatant (= adsorbed plasma) was stored in 1 ml fractions at -20°C.

Table 2: Characteristics of tSCI patients used in the serological antigen selection procedure

Patient	Time of sampling ^a	Age ^b	Gender ^c	ASIA ^d	Location of injury ^e	Type of injury
1	T1	74	F	D	C1	Compression
2	T1	29	M	A	C4	Contusion
3	T1	85	M	B	C6	Contusion
4	T1	34	M	NA ^f	C6-T2	Contusion
5	T0	28	M	A	T5	Laceration
6	T0	68	M	C	NA	Compression
7	T0	44	M	D	C4-5	Contusion
8	T0	39	M	NA	C4-6	Contusion
9	T0	31	M	NA	T6-10	NA
10	T0	55	M	NA	C6	NA

^a T0=at admission, T1=3 weeks after SCI

^b in years

^c F=female, M=male

^d ASIA=American Spinal Injury Association classification

^e C=cervical level, T=thoracal level,

^f NA=not available

2.4 Serological antigen selection

Plasma of 10 tSCI patients (Table 2) was used to perform the SAS procedure. Immunotubes (Nunc, Roskilde, Denmark) were coated with 10 µg/ml rabbit anti-human IgG (Dako, Glostrup, Denmark) in 0.1 M NaHCO₃ (pH 9.6). After overnight incubation at 4°C, immunotubes were washed with 0.1% (v/v) PBS-Tween 20 and PBS (two times). Subsequently, tubes were blocked with 2% (w/v) Marvel-PBS (MPBS) (2 h, room temperature (RT)). A pre-incubation mixture was made by adding diluted pre-adsorbed plasma (1:100 in 0.1% MPBS) to equal amounts of phage (ca. 10¹²-10¹³ plaque forming units (pfu)) from every library or output from the previous selection round in a glass tube.

The mixture was incubated for 1.5 h at RT in an end-over-end rotor. After blocking, immunotubes were washed two times with 0.1% (v/v) PBS-Tween 20 and two times with PBS and the pre-incubation mixture was transferred to the immunotube for 30 min on an end-over-end rotor and 2 h standing (both at RT). Immunotubes were washed 20 times with 0.1% (v/v) PBS-Tween 20 and 20 times with PBS to discard non-bound phage. Bound phage were eluted with 1 ml 100 mM triethylamide (pH 12, 10 min, rotor, RT) and neutralized in 0.5 ml 1M Tris-HCl (pH 7.4). A titration of input and output phage was performed at each selection round by infection of TG1 *E. Coli cells* ($OD_{600}=0.7$) and grown overnight at 30°C on 2xYTAG plates. Subsequently, an amplification of the output phage was performed by infection of *E. coli* TG1 cells with 1 ml output. After centrifugation (10 min, 4000 rpm), the pellet was resuspended in 2xTYAG medium and grown overnight on 2xYTAG plates at 30°C. Amplification plates were scraped, glycerol stocks were made (15% glycerol) and stored at -80°C. After amplification, phage were isolated for further affinity selection rounds. The output was characterized by PCR, restriction digestion and sequencing experiments (see section 2.1.4).

3 Results

3.1 Construction of a primary hSC library

To investigate the antibody response after SCI via the SAS procedure, hSC cDNA phage display libraries were developed from commercially obtained normal hSC Poly A+ RNA. An initial quality control of the obtained Poly A+ RNA was performed by denaturing agarose gel electrophoresis. Results (not shown) indicated a size range from 0.2 to 10 kb. This broad size range indicates a high diversity of the RNA. 5 µg Poly A+ RNA was subsequently converted to double-stranded cDNA. Samples from the first (single stranded cDNA) and second-strand (double stranded cDNA) synthesis were separated by gel electrophoresis to evaluate the efficiency of both synthesis reactions (Figure 5a). After gel electrophoresis, a smear was visible for both synthesis steps. Since for both cDNA synthesis reactions a same pattern was present, we assumed that conversion of the total Poly A+ RNA had taken place. The obtained double-stranded cDNA fragments were ligated with an EcoRI and XhoI adapter (Figure 3a). Subsequently, a column chromatography was performed to fractionate the cDNA fragments into 20 fractions. From these 20 fractions, fractions 1 until 12 were pooled to use for the ligation. The selected fractions had the highest concentration, indicating that larger cDNA fragments were present in these fractions. The column chromatography was also used to remove residual adapters.

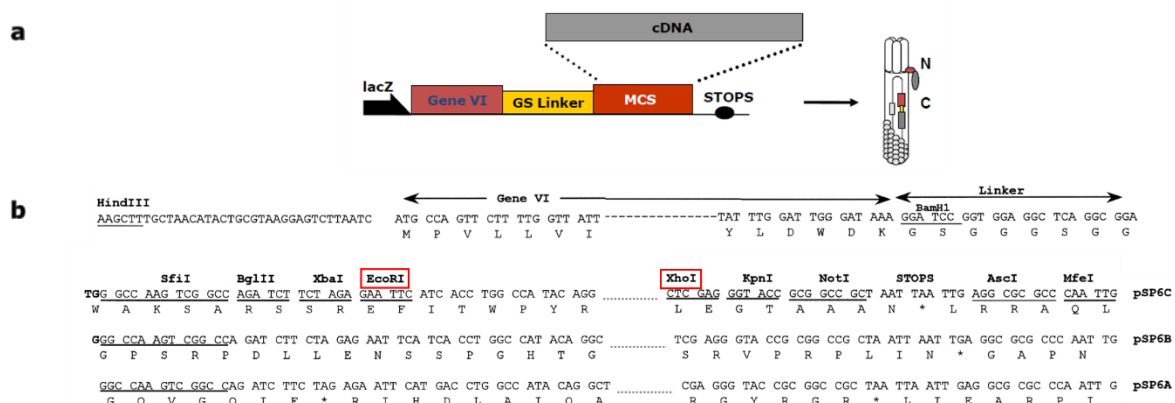


Figure 4: Phage display vectors (pSPVI-system) (45). (a) The ligation construct consisted of a lacZ promoter that initiates transcription, a GS linker which separates the pVI gene from the cloned cDNA and gene VI which makes fusion of the cDNA fragments to the C-terminus of minor coat protein VI possible. (b) Sequences of the three pSPVI phage display vectors (pSPVIA/B/C), which differ one or two nucleotides from each other. Three phage display vectors were used to allow expression of the cDNA inserts in all three reading frames. All three phage display vectors were restricted with EcoRI and XhoI, which allowed ligation of the EcoRI/XhoI adapted hSC cDNA in the three phage display vectors. The used restriction enzymes are framed in red. N = N-terminus, C = C-terminus, GS = glycine/serine linker, MCS = multiple cloning site

hSC cDNA inserts were ligated in a 1:20 ratio (vector:insert) in cDNA phage display vector pSPVIC (Figure 4) and electroporated into electrocompetent TG1 *E. coli* cells (Figure 3b) to obtain a primary hSC library. The primary hSC library had a recombination efficiency of 83.63% and insert sizes ranged between 300 bp (empty vector) and 1600 bp (Figure 5b). hSC inserts between 300 bp and

600 bp were most abundant (Figure 5c). Randomly chosen colonies were fingerprinted with BstNI to check if cDNA inserts that had the same length also represent inserts with a similar sequence. cDNA inserts of the same length had different restriction patterns (Figure 5d, digested inserts are indicated with a red asterisk), indicating that these inserts most likely represent different cDNA inserts. These findings confirm the diversity of the library. Digestion of 100 times the primary library size with EcoRI and XhoI resulted in the pSPVIC vector at 3500 bp and hSC cDNA inserts ranging from <100 bp until 3500 bp (Figure 5e), which confirms that also large inserts were ligated.

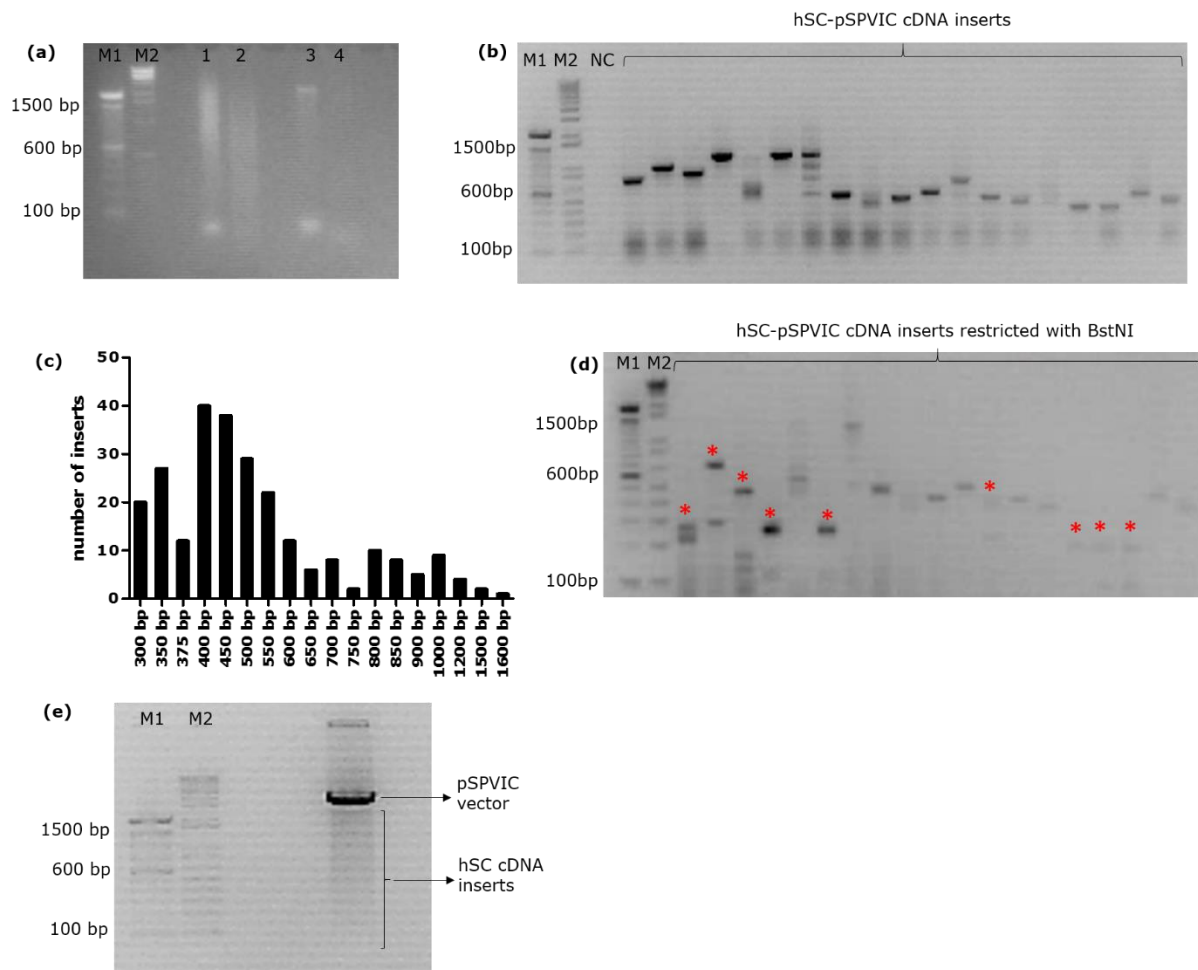


Figure 5: Primary hSC library. (a) Analysis of the first-strand (1) and second-strand (2) cDNA synthesis by gel electrophoresis. Clear smears with a similar pattern were visible in lane 1 and 2, indicating that both synthesis reactions allowed conversion of the total Poly A+ RNA. Lane 3 and 4 were loaded with first-strand (3) and second-strand (4) control cDNA, which was enclosed in the SuperScript Choice System for cDNA synthesis kit. (b) Colony PCR was performed using primers that bind adjacent to the cDNA inserts. A broad range of hSC cDNA insert sizes were present. (c) Distribution of the insert sizes present in the primary hSC cDNA library. The insert size ranged from 300 bp to 1600 bp based on gel electrophoresis analysis. A band of 300 bp indicates that no insert was ligated into the vector. (d) Fingerprinting of the hSC pSPVIC inserts. BstNI was used to perform a fingerprinting on colony PCR samples (the same samples as in (d)). Red asterisk indicate that BstNI has cut the sample. (e) Restriction of the primary hSC cDNA library with XhoI and EcoRI. The pSPVIC vector can be seen at 3500 bp and hSC cDNA inserts varied between 100 bp and 3500 bp. M1 = 100 bp marker, M2 = 1 kb marker, NC = negative control (no template), bp = base pairs

3.2 Characterization and identification of the hSC libraries in a pSPVI vector system

The primary hSC library (hSC-pSPVIC) was amplified and digested with EcoRI and XhoI. The resulting hSC inserts were ligated into phage display vector pSPVIA and B (Figure 4). Subsequently, the ligation mixtures were transformed into electrocompetent *E. coli* TG1 cells to obtain hSC-pSPVIA and B libraries (Figure 3c).

In order to cover all rare genes, a library with at least 10^6 recombinants needed to be developed since 10^4 - 10^5 different genes are present in an average mammalian cell (45). The primary diversity of the three hSC cDNA libraries were determined (Table 3). All three hSC cDNA libraries had a primary diversity higher than 10^6 cfu (diversity hSC-pSPVIA: 7.8×10^6 cfu, hSC-pSPVIB: 1.4×10^6 cfu and hSC-pSPVIC: 2.6×10^6 cfu). After amplification, the concentration of the hSC cDNA libraries was determined by a titration (Table 3). The titers of all three hSC cDNA libraries were in the same range, 2×10^{10} cfu/ml.

Table 3: Primary diversity and titer of hSC-pSPVIA, B and C libraries

Library	Primary diversity^a	Titer^b
hSC-pSPVIA	7.8×10^6	2.1×10^{10}
hSC-pSPVIB	1.4×10^6	2×10^{10}
hSC-pSPVIC	2.6×10^6	2.4×10^{10}

^a Diversity is depicted in cfu

^b Titer is depicted in cfu/ml

From each hSC library, individual colonies were used to perform a colony PCR, which was analyzed by gel electrophoresis and showed the presence of a broad range of cDNA inserts. The wide range of cDNA insert sizes indicates that the diversity of the primary hSC cDNA library was conserved in the hSC-pSPVIA (Figure 6a) and B libraries (Figure 6c). The percentage of recombination for the hSC-pSPVIA and B libraries were respectively 93.19% and 96.94%. A fingerprinting was performed on several colony PCR samples from the hSC-pSPVIA (Figure 6b) and B library (Figure 6d) by using the restriction enzyme BstNI (restricted samples are indicated with a red asterisk).

Sequencing was performed on purified colony PCR samples of each library (Supplementary table 1) to evaluate the diversity, the cloning construct and the identity of the libraries. Nucleotide sequence matches were searched with the basic local alignment search tool of NCBI (<http://blast.ncbi.nlm.nih.gov/Blast.cgi>), gene matches were found on cDNA level. Besides the identification of known and characterized proteins, one sequence encoded for a protein with an unidentified function. Only one sequenced cDNA insert contained no insert, indicating the high quality of the libraries. The majority of gene matches were located in the 3' untranslated region (3' UTR), which is caused by the use of an oligo(dT) primer during the conversion of hSC poly A+ RNA in cDNA. The cellular location of the gene match encoded proteins were determined on Universal Protein Resource (UniProt, <http://www.uniprot.org/>). The majority of protein matches were located in the cytoplasm, nucleus and cellular membrane (Figure 7, Supplementary table 1). Nuclear proteins that

were found are involved in transcriptional (e.g. transcription factor binding to IGHM enhancer 3), RNA (e.g. transcription factor IIIC) and DNA (e.g. MRE11 meiotic recombination 11 homolog A) processes. Protein matches present in the cytoplasm play a role in cell signaling, cellular transport (e.g. alstrom syndrome 1)), cell growth and proliferation (e.g. ribosomal protein S6), inhibition and activation of certain proteins (e.g. calpain), apoptosis (e.g. cell division cycle associated 7), etc. Processes that are linked to proteins at the cellular membrane are transport (e.g. chloride intracellular channel 6) and immunity (e.g. leukocyte specific transcript 1).

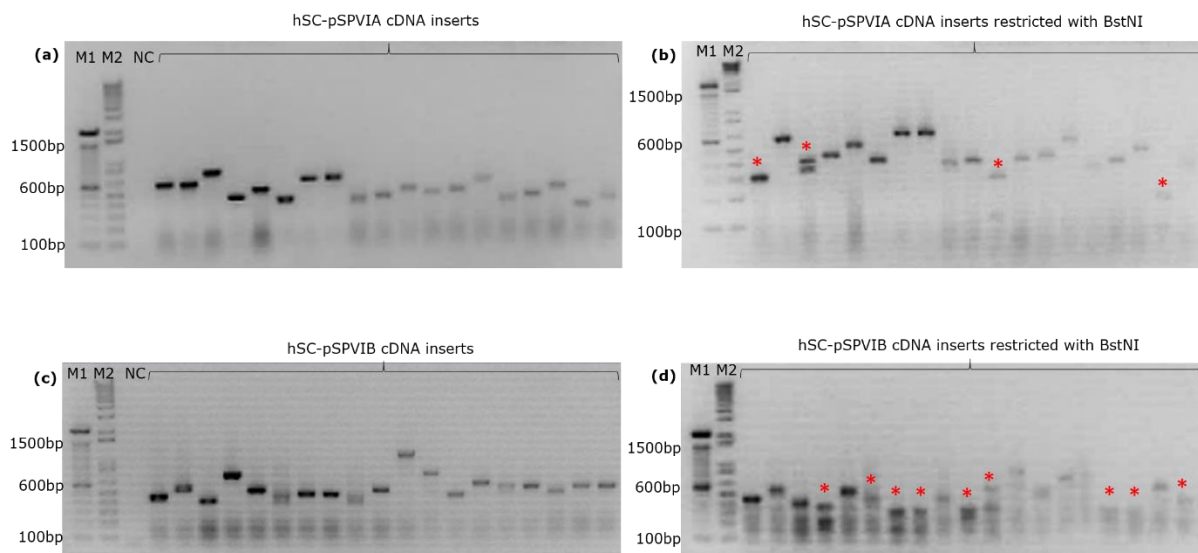


Figure 6: Diversity of hSC-pSPVIA and B cDNA library. Colony PCR using primers that bind adjacent to the cDNA inserts was performed on the hSC-pSPVIA (a) and hSC-pSPVIB (c) library. A broad range of hSC cDNA insert sizes were present. Fingerprinting of the hSC-pSPVIA (b) and hSC-pSPVIB (d) inserts. BstNI was used to perform a fingerprinting on colony PCR samples (the same samples as in (a) and (c)). Red asterisks indicate that BstNI has digested the sample. M1 = 100 bp marker, M2 = 1 kb marker, NC = negative control (no template), bp = base pairs

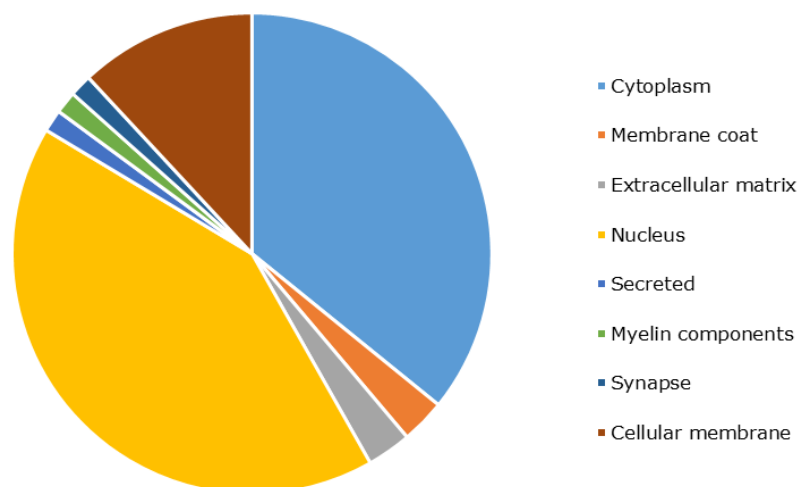


Figure 7: Identity of cDNA phage display libraries. Sequencing of randomly chosen hSC inserts were blasted on NCBI using BLAST. Cellular locations of the gene match encoded proteins were searched on UniProt. The graph shows the cellular distribution of the gene match encoded proteins. Gene matches were especially located in the nucleus, cytoplasm and cellular membrane.

3.3 Screening of hSC cDNA libraries

In order to identify novel candidate antibody biomarkers in SCI pathology, SAS is used (Figure 2). The three hSC phage display libraries were screened for antibody reactivity using pooled plasma of 10 tSCI patients (Table 2). These patients were mainly young adult men with a varying ASIA classification and location and type of injury (Table 2), which represents the actual tSCI patient population. During the SAS procedure, antigen-antibody complexes were captured, eluted and amplified. Several selection rounds with the same plasma pool have been performed to enrich relevant phage (44). After each selection round the titer of input and output phage was determined (Table 4). Every selection round was started with an input phage titer of 10^{13} cfu/ml, which indicated that the functionality of the phage was intact. After the first and second round a decrease of the titer until 10^4 cfu/ml could be observed. From the second round of selection onwards a gradual increase of the titer was noticed.

Table 4: Selection of pVI phage displayed hSC cDNA library on tSCI patient plasma

Round	Input ^a	Output ^a
1	4.35×10^{13}	7.6×10^4
2	3.27×10^{13}	5.6×10^4
3	3.9×10^{13}	6×10^5
4	5.24×10^{13}	8.05×10^6

^a Titer of input and output phage is shown in cfu/ml

After four rounds of selection, colony PCR and restriction digestions were performed on 240 randomly selected cDNA inserts. Colony PCR analysis showed that cDNA insert sizes ranged between 300 bp and 2000 bp, indicating that still a lot of variation in cDNA inserts is present. It also demonstrated that some enrichment took place for cDNA inserts with a length of 500 bp, 650 bp and 800 bp (Figure 8a and b). The agarose gel of the fingerprinting on the colony PCR samples by BstNI show two cDNA inserts with the same restriction pattern (Figure 8c), however in general the restriction patterns differ from each other. The different restriction patterns demonstrated that there was no enrichment of specific inserts. These findings show that after four rounds of selection no enrichment was present, implicating that a fifth round needs to be performed with modified selection conditions.

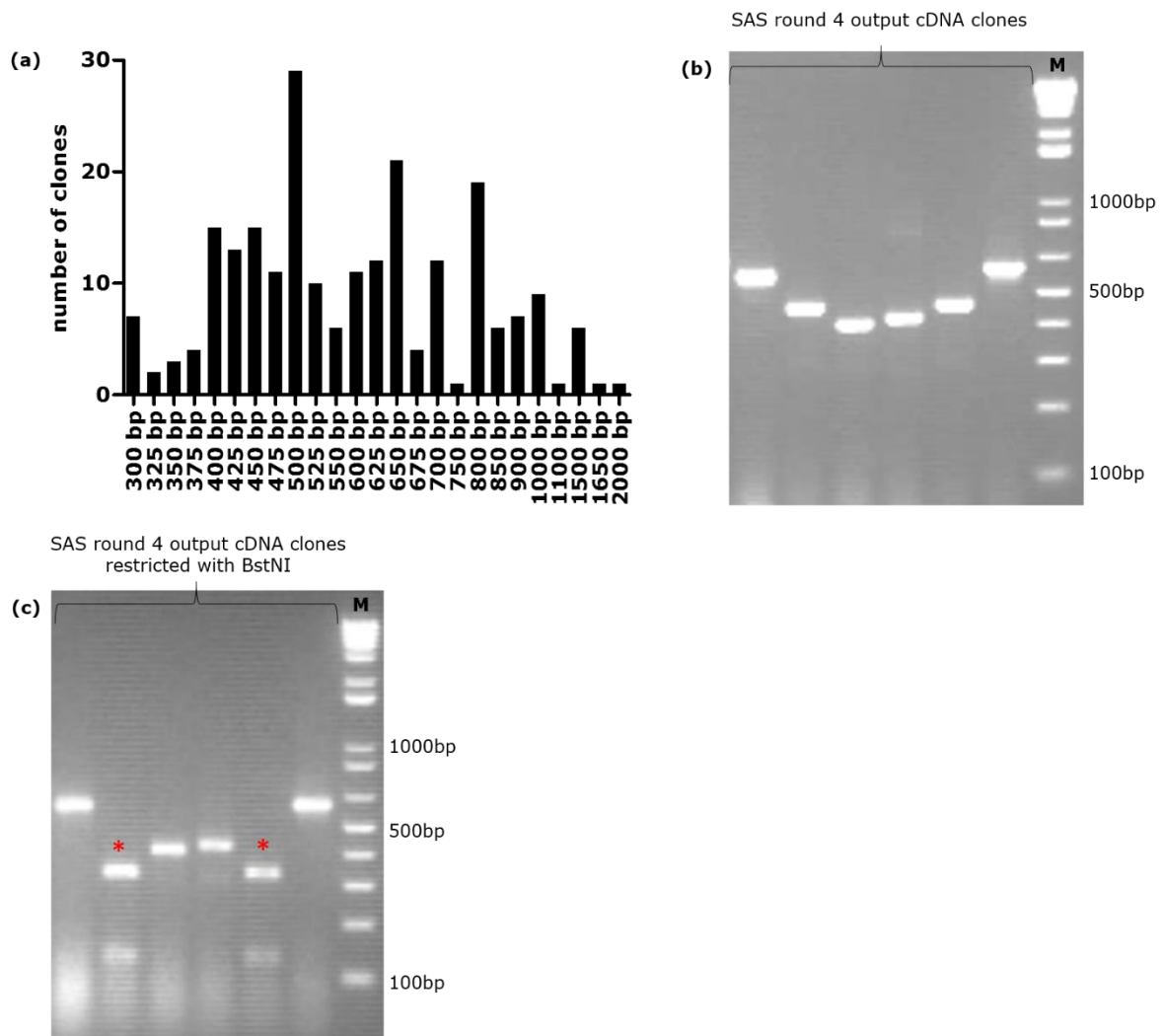


Figure 8: Analysis of SAS output round 4. (a) Distribution of the lengths of cDNA inserts after the fourth SAS, based on gel electrophoresis. The size of the inserts ranged between 300 bp and 2000 bp, showing that still a lot of variation in cDNA inserts is present. A high number of inserts with a length of 500 bp, 650 bp and 800 bp were present. (b) Colony PCR using primers that bind adjacent to the cDNA inserts was performed on the output of the fourth SAS round. Bands on several heights were present. (c) BstNI was used to perform a fingerprinting on colony PCR samples of the output of fourth selection round (the same samples as in (b)). Red asterisks indicate that BstNI has digested the sample. Two inserts had the same restriction pattern, which may indicate that this are the same inserts. M = 1 kb marker, bp = base pairs

4 Discussion

SCI is a devastating condition, which is caused by trauma. Some potential biomarkers were already studied in animal and human studies, but they did not lead to a reliable biomarker for SCI. A reliable antibody biomarker for SCI would be interesting because autoantibodies are produced after SCI and aggravate the initial lesion (29, 30). The targets of these SCI-induced autoantibodies can be determined and can lead to more insights into the underlying disease processes of SCI, which could contribute to an improved diagnosis and prognosis and novel or severity-specific therapies. Blood samples can be used to investigate the antibody response, which is less invasive than a lumbar puncture to obtain cerebrospinal fluid. Antibody biomarkers can be discovered using a variety of techniques (e.g. proteome arrays, peptide phage display, etc.). During this study the SAS procedure was the preferred method of choice due to the effectiveness of this technique to study antibody reactions. SAS has already been used in our research team to identify novel candidate antibody biomarkers for multiple sclerosis (40), rheumatoid arthritis (41) and clinical isolated syndrome (42).

hSC cDNA libraries were developed using poly A+ RNA derived from normal spinal cords. We have chosen to work with normal spinal cord tissue, because animal studies showed that an injection of purified antibodies from SCI mice into healthy spinal cord tissue of WT mice induced persistent paralysis and SCI pathology (30). This research confirmed that neuroinflammation which occurs after a SCI also affects the healthy tissue surrounding the initial lesion and antibodies directed against healthy tissue are present after SCI. However, targets that are present in damaged spinal cord tissue can be missed, because healthy tissue does not display the entire inflammatory antigen composition (44).

Quality control of the hSC polyA+ RNA revealed a size range between 0.2 and 10 kb (result not shown), which showed the high diversity of the RNA template. hSC poly A+ RNA was converted to double-stranded cDNA by first and second-strand synthesis. Gel electrophoresis of cDNA from the first and second-strand synthesis revealed cDNA fragments ranging from approximately <0.1 kb until 10 kb (Figure 5a), indicating that the diversity was conserved during the cDNA synthesis. The double-stranded cDNA was provided with a XhoI and EcoRI adapter (Figure 3a), to allow expression in the correct orientation (45).

The ligation reaction was evaluated by random colony PCR (Figure 5b) and fingerprinting (Figure 5d). Colony PCR analysis resulted in 83.63% recombination and insert sizes ranged between 300 bp and 1600 bp, indicating that cDNA fragments up to 1600 bp were ligated into the vector. However, the majority of insert lengths were between 300 bp and 600 bp (Figure 5c). A high variety of restriction patterns from the fingerprinted hSC cDNA inserts was present, meaning that different cDNA inserts are ligated confirming the high diversity of the primary hSC library (Figure 5d). The diversity of the primary hSC cDNA library was confirmed by digestion of 100 times the library size with EcoRI and XhoI (Figure 5e), showing that cDNA inserts with a length of more than 1600 bp were ligated into the vector. To obtain a diverse cDNA library and a higher amount of coding cDNA fragments that makes the characterization easier, the presence of large inserts was preferred.

In order to have the correct reading frame for every hSC cDNA insert three phage display vectors were used (Figure 4). These vectors allow fusion of cDNA inserts to the C-terminus of gene VI. This

has the advantage that full length expression of cDNA fragments is possible and stop codons do not prevent the display of cDNA inserts. Another advantage is the presence of one cDNA encoded protein/peptide per phage particle, leading to high affinity interactions during antibody selections. The use of two different adapters, three phage display vectors and fusion to the c-terminus of phage coat protein pVI ensured that the correct expression of the cDNA insert was present in the hSC cDNA libraries (45, 46).

hSC cDNA inserts were isolated from the primary hSC library and purified to ligate into phage display vectors pSPVIA and B. After electroporation into *E. coli* TG1 electrocompetent cells, hSC-pSPVIA and B cDNA libraries were obtained (Figure 3c). Colony PCR and fingerprinting experiments showed that the diversity of the primary hSC cDNA library was conserved (Figure 6). The primary diversity of all three hSC cDNA libraries was higher than 10^6 cfu and the titer was in the range of 2×10^{10} cfu/ml (Table 3).

hSC cDNA inserts were sequenced in order to check the cloning construct, diversity and content of every library. Cellular location of the gene match encoded proteins were determined on UniProt (Supplementary table 1). Analysis of the cellular distribution revealed that the majority of gene match encoded proteins are located in the cytoplasm, nucleus and cellular membrane (Figure 7). Proteins located in the nucleus play a role in transcriptional, RNA and DNA processes. Cytoplasmic proteins are involved in cell growth, proliferation, cell signaling, cellular transport, apoptosis, inhibition and activation of certain proteins, etc. Proteins that play a role in transport processes and the immune response are located in the cellular membrane. The highest corresponding nucleotide sequence matches contribute to different processes at different cellular locations, which implies that a diverse group of proteins/peptides are expressed. However, most cDNA fragments correspond to the 3' UTR of the matching gene, which was caused by the use of an oligo(dT) primer. A possible solution to increase the number of coding cDNA fragments could be the use of random primers. A disadvantage of these 3' UTR marching cDNA sequences is that it favors the identification of mimotopes. Mimotopes structurally mimic the authentic *in vivo* antigens by forming epitopes, implying that the mimotope and the actual antigen are not automatically comparable at the amino-acid level. Mimotopes make the identification and characterization of the real antigen labor-intensive (44).

To express the ligated hSC cDNA inserts on the surface of filamentous phage, the hSC-pSPVIA, B and C libraries were infected with M13K07 helper phage (Figure 3c). These phage display libraries were screened for antibody reactivity with a pool of plasma samples derived from 10 tSCI patients (Table 2). This patient subpopulation consisted mainly of young adult men with varying ASIA classification and location and type of injury. The heterogeneous characteristics of this subpopulation are comparable with the general patient population (2, 3). Blood samples at admission (T0 sample) and three weeks after SCI (T1 sample) were obtained. T0 samples were used to search for acute biomarkers. Three weeks after SCI newly formed antibody responses appear due to interaction of the immune system with CNS antigens. The use of the T1 sample was also preferred because we focus on IgG responses, which have their peak concentration at 10 – 14 days after first antigen

exposure (47). Furthermore, IgG antibodies have an average biological half-life of 21 days (48). The use of the T1 sample leads to the detection of newly formed antibody reactions.

SAS uses phage display, which is an easy and rapid selection method for screening of candidate antigens and could lead to the identification of unknown proteins/peptides (46, 49). After each selection round the titer of the input and output phage was determined (Table 4). An input titer of 10^{13} cfu/ml was reached in the beginning of every selection, indicating that the functionality of the phage was intact. After the first and second selection round, the output titer was decreased until 10^4 cfu/ml. A gradual increase of the output titer starting from the second round indicated an enrichment of phage clones. After the fourth round of selection, colony PCR and fingerprinting (Figure 8) of 240 randomly chosen clones indicated that no enrichment occurred. Colony PCR analysis revealed that cDNA fragments varied between 300 bp and 2000 bp after the fourth round of selection. cDNA fragments of 500 bp, 650 bp and 800 bp were most abundant (Figure 8a). Fingerprinting of random PCR products resulted in digested cDNA fragments, but did not indicate enrichment of specific cDNA clones. Although a very low amount of cDNA fragments showed a similar restriction pattern (Figure 8b and c). These results indicate that a fifth selection round needs to be performed with modified selection conditions. If the fifth SAS round does not lead to enriched phage, a negative selection round using healthy control plasma could be performed.

In conclusion, we successfully made hSC cDNA libraries, which were displayed on the surface of filamentous phage by fusion to phage coat protein pVI. These phage libraries were screened for antibody reactivity by using plasma of 10 tSCI patients. Four screening rounds were performed, so far no enrichment of cDNA clones could be observed. Therefore, a fifth selection round needs to be performed with modified selection conditions, such as more wash steps and a lower coating concentration of anti-human IgG.

In the future, the relevance of these potential antibody biomarkers will be studied in the pathology of human SCI by performing a screening on plasma samples from SCI patients and healthy controls. By using a phage enzyme-linked immunosorbent assay (ELISA), potential antibody biomarkers will also be explored for their role in SCI pathology and their diagnostic, prognostic and theranostic relevance in SCI. Correlations between the antibody response and clinical parameters will be determined. Next, the most promising antibody biomarkers need to be validated, which will be done by confirming the presence of these markers in a large number of SCI patients. Furthermore, these potential antibody biomarkers need to be characterized further to determine the identity of the corresponding antigens. The identity can be determined by performing an immunoprecipitation followed by western blotting and mass spectrometry of the newly found biomarkers. Knowing the identity of the corresponding antigens can lead to a better understanding of SCI pathology. The sensitivity and specificity of these biomarkers has to be determined to see if they are accurate enough to be used in clinical settings. Since SAS allows the development of sensitive high-throughput binding assays, an ELISA can be developed to commercialize the antibody biomarkers with the highest sensitivity.

5 References

1. McDonald JW, Sadowsky C. Spinal-cord injury. *Lancet*. 2002;359(9304):417-25.
2. Burt AA. The epidemiology, natural history and prognosis of spinal cord injury. *Current Orthopaedics*. 2004;18(1):26-32.
3. Spinal cord injury facts and figures at a glance. *J Spinal Cord Med*. 2013;36(5):568-9.
4. Yokobori S, Zhang Z, Moghieb A, Mondello S, Gajavelli S, Dietrich WD, et al. Biomarkers for spinal cord injury. 2013.
5. Lee BB, Cripps RA, Fitzharris M, Wing PC. The global map for traumatic spinal cord injury epidemiology: update 2011, global incidence rate. *Spinal Cord*. 2014;52(2):110-6.
6. Furlan J, Krassioukov A, Miller W, Sakakibara B. Epidemiology of Traumatic SCI. *Spinal Cord Injury Rehabilitation Evidence*. 2012;4.0:1-16.
7. Wyndaele M, Wyndaele JJ. Incidence, prevalence and epidemiology of spinal cord injury: what learns a worldwide literature survey? *Spinal Cord*. 2006;44(9):523-9.
8. Dryden DM, Saunders LD, Rowe BH, May LA, Yiannakoulias N, Svenson LW, et al. Utilization of health services following spinal cord injury: a 6-year follow-up study. *Spinal Cord*. 2004;42(9):513-25.
9. Maynard FM, Bracken MB, Creasey G, Ditunno JF, Donovan WH, Ducker TB, et al. International Standards for Neurological and Functional Classification of Spinal Cord Injury. American Spinal Injury Association. *Spinal Cord*. 1997;35(5):266-74.
10. Lammertse D, Dungan D, Dreisbach J, Falci S, Flanders A, Marino R, et al. Neuroimaging in traumatic spinal cord injury: an evidence-based review for clinical practice and research. *J Spinal Cord Med*. 2007;30(3):205-14.
11. Yokobori S, Zhang Z, Moghieb A, Mondello S, Gajavelli S, Dietrich WD, et al. Acute Diagnostic Biomarkers for Spinal Cord Injury: Review of the Literature and Preliminary Research Report. *World Neurosurg*. 2013.
12. Pouw MH, Hosman AJF, van Middendorp JJ, Verbeek MM, Vos PE, van de Meent H. Biomarkers in spinal cord injury. *Spinal Cord*. 2009;47(7):519-25.
13. van Middendorp JJ, Hosman AJ, Donders AR, Pouw MH, Ditunno JF, Curt A, et al. A clinical prediction rule for ambulation outcomes after traumatic spinal cord injury: a longitudinal cohort study. *Lancet*. 2011;377(9770):1004-10.
14. Furlan JC, Bracken MB, Fehlings MG. Is age a key determinant of mortality and neurological outcome after acute traumatic spinal cord injury? *Neurobiology of Aging*. 2010;31(3):434-46.
15. Seel RT, Huang ME, Cifu DX, Kolakowsky-Hayner SA, McKinley WO. Age-related differences in length of stays, hospitalization costs, and outcomes for an injury-matched sample of adults with paraplegia. *J Spinal Cord Med*. 2001;24(4):241-50.
16. Wilson JR, Grossman RG, Frankowski RF, Kiss A, Davis AM, Kulkarni AV, et al. A clinical prediction model for long-term functional outcome after traumatic spinal cord injury based on acute clinical and imaging factors. *J Neurotrauma*. 2012;29(13):2263-71.
17. Haisma JA, van der Woude LH, Stam HJ, Bergen MP, Sluis TA, Post MW, et al. Complications following spinal cord injury: occurrence and risk factors in a longitudinal study during and after inpatient rehabilitation. *J Rehabil Med*. 2007;39(5):393-8.
18. Hurlbert RJ. Methylprednisolone for acute spinal cord injury: an inappropriate standard of care. *J Neurosurg*. 2000;93(1 Suppl):1-7.
19. Short DJ, El Masry WS, Jones PW. High dose methylprednisolone in the management of acute spinal cord injury - a systematic review from a clinical perspective. *Spinal Cord*. 2000;38(5):273-86.
20. Sayer FT, Kronvall E, Nilsson OG. Methylprednisolone treatment in acute spinal cord injury: the myth challenged through a structured analysis of published literature. *Spine J*. 2006;6(3):335-43.
21. Silva NA, Sousa N, Reis RL, Salgado AJ. From basics to clinical: a comprehensive review on spinal cord injury. *Prog Neurobiol*. 2014;114:25-57.
22. Thuret S, Moon LD, Gage FH. Therapeutic interventions after spinal cord injury. *Nat Rev Neurosci*. 2006;7(8):628-43.
23. Dekaban GA, Thawer S. Pathogenic antibodies are active participants in spinal cord injury. *Journal of Clinical Investigation*. 2009;119(10):2881-4.
24. Nguyen DH, Cho N, Satkunendrarajah K, Austin JW, Wang J, Fehlings MG. Immunoglobulin G (IgG) attenuates neuroinflammation and improves neurobehavioral recovery after cervical spinal cord injury. *Journal of Neuroinflammation*. 2012;9:14.
25. Fehlings MG, Nguyen DH. Immunoglobulin G: A Potential Treatment to Attenuate Neuroinflammation Following Spinal Cord Injury. *Journal of Clinical Immunology*. 2010;30:S109-S12.

26. Popovich PG, Stokes BT, Whitacre CC. Concept of autoimmunity following spinal cord injury: possible roles for T lymphocytes in the traumatized central nervous system. *J Neurosci Res.* 1996;45(4):349-63.
27. Jones TB, Basso DM, Sodhi A, Pan JZ, Hart RP, MacCallum RC, et al. Pathological CNS autoimmune disease triggered by traumatic spinal cord injury: implications for autoimmune vaccine therapy. *J Neurosci.* 2002;22(7):2690-700.
28. Ankeny DP, Popovich PG. B cells and autoantibodies: complex roles in CNS injury. *Trends in Immunology.* 2010;31(9):332-8.
29. Ankeny DP, Lucin KM, Sanders VM, McGaughy VM, Popovich PG. Spinal cord injury triggers systemic autoimmunity: evidence for chronic B lymphocyte activation and lupus-like autoantibody synthesis. *Journal of Neurochemistry.* 2006;99(4):1073-87.
30. Ankeny DP, Guan Z, Popovich PG. B cells produce pathogenic antibodies and impair recovery after spinal cord injury in mice. *Journal of Clinical Investigation.* 2009;119(10):2990-9.
31. Lucin KM, Sanders VM, Jones TB, Malarkey WB, Popovich PG. Impaired antibody synthesis after spinal cord injury is level dependent and is due to sympathetic nervous system dysregulation. *Experimental Neurology.* 2007;207(1):75-84.
32. Hayes KC, Hull TCL, Delaney GA, Potter PJ, Sequeira KAJ, Campbell K, et al. Elevated serum titers of proinflammatory cytokines and CNS autoantibodies in patients with chronic spinal cord injury. *Journal of Neurotrauma.* 2002;19(6):753-61.
33. Mizrachi Y, Ohry A, Aviel A, Rozin R, Brooks ME, Schwartz M. SYSTEMIC HUMORAL-FACTORS PARTICIPATING IN THE COURSE OF SPINAL-CORD INJURY. *Paraplegia.* 1983;21(5):287-93.
34. Davies AL, Hayes KC, Dekaban GA. Clinical correlates of elevated serum concentrations of cytokines and autoantibodies in patients with spinal cord injury. *Archives of Physical Medicine and Rehabilitation.* 2007;88(11):1384-93.
35. Vaage J, Anderson R. Biochemical markers of neurologic injury in cardiac surgery: the rise and fall of S100beta. *J Thorac Cardiovasc Surg.* 2001;122(5):853-5.
36. Guéz M, Hildingsson C, Rosengren L, Karlsson K, Toolanen G. Nervous tissue damage markers in cerebrospinal fluid after cervical spine injuries and whiplash trauma. *J Neurotrauma.* 2003;20(9):853-8.
37. Kwon BK, Stammers AM, Belanger LM, Bernardo A, Chan D, Bishop CM, et al. Cerebrospinal fluid inflammatory cytokines and biomarkers of injury severity in acute human spinal cord injury. *J Neurotrauma.* 2010;27(4):669-82.
38. Hayakawa K, Okazaki R, Ishii K, Ueno T, Izawa N, Tanaka Y, et al. Phosphorylated neurofilament subunit NF-H as a biomarker for evaluating the severity of spinal cord injury patients, a pilot study. *Spinal Cord.* 2012;50(7):493-6.
39. Pouw MH, Kwon BK, Verbeek MM, Vos PE, van Kampen A, Fisher CG, et al. Structural biomarkers in the cerebrospinal fluid within 24 h after a traumatic spinal cord injury: a descriptive analysis of 16 subjects. *Spinal Cord.* 2014.
40. Somers V, Govarts C, Somers K, Hupperts R, Medaer R, Stinissen P. Autoantibody profiling in multiple sclerosis reveals novel antigenic candidates. *J Immunol.* 2008;180(6):3957-63.
41. Somers K, Geusens P, Elewaut D, De Keyser F, Rummens JL, Coenen M, et al. Novel autoantibody markers for early and seronegative rheumatoid arthritis. *J Autoimmun.* 2011;36(1):33-46.
42. Rouwette M, Noben JP, Van Horssen J, Van Wijmeersch B, Hupperts R, Jongen PJ, et al. Identification of coronin-1a as a novel antibody target for clinically isolated syndrome and multiple sclerosis. *J Neurochem.* 2013;126(4):483-92.
43. Somers V, Govarts C, Hellings N, Hupperts R, Stinissen P. Profiling the autoantibody repertoire by serological antigen selection. *Journal of Autoimmunity.* 2005;25(3):223-8.
44. Somers K, Stinissen P, Somers V. Optimization of High-throughput Autoantibody Profiling for the Discovery of Novel Antigenic Targets in Rheumatoid Arthritis. *Contemporary Challenges in Autoimmunity.* 2009;1173:92-102.
45. Hufton SE, Moerkerk PT, Meulemans EV, de Bruïne A, Arends JW, Hoogenboom HR. Phage display of cDNA repertoires: the pVI display system and its applications for the selection of immunogenic ligands. *J Immunol Methods.* 1999;231(1-2):39-51.
46. Somers K, Govarts C, Stinissen P, Somers V. Multiplexing approaches for autoantibody profiling in multiple sclerosis. *Autoimmun Rev.* 2009;8(7):573-9.
47. K.A. A, H.A. L. Humoral immune responses. Third ed. Philadelphia: Saunders Elsevier; 2011.
48. Morell A, Terry WD, Waldmann TA. Metabolic properties of IgG subclasses in man. *J Clin Invest.* 1970;49(4):673-80.
49. Somers VA, Brandwijk RJ, Joosten B, Moerkerk PT, Arends JW, Menheere P, et al. A panel of candidate tumor antigens in colorectal cancer revealed by the serological selection of a phage displayed cDNA expression library. *J Immunol.* 2002;169(5):2772-80.

6 Supplementary

Supplementary table 1: Identity of hSC-pSPVIA/B/C cDNA inserts

Clone	Nucleotide sequence	Homology on nucleotide level	Coding	Cellular component
hSC 1	CCTCCTCACAGAGGAGAGGGCCTGTGGTCTGTAGAAGGTAA (42)	98% (41/42, e = 3 ⁻¹¹) Homo sapiens C15orf38-AP3S2 readthrough (C15orf38-AP3S2), mRNA	3' UTR	Membrane coat
		98% (41/42, e = 3 ⁻¹¹) Homo sapiens adaptor-related protein complex 3, sigma 2 subunit (AP3S2), transcript variant 1, mRNA	3' UTR	Golgi apparatus
hSC 2	CAGAAGGGCTATGGATTAGTTTGA (24)	100% (24/24, e=8 ⁻⁰⁶) Homo sapiens signal recognition particle 9kDa (SRP9), transcript variant 1-2, mRNA	3' UTR	Cytoplasm
hSC 3	GAGTTTTACAGTTATAACCACTGGGATTGTGAGACCATAGGACATTTGAACAATCTTTTCTTCTACCCATCTAGAAAAGCATCTTTTTTATATACCAAATTTTTACACATATATCCACATCTGTTTTGAAATCTAGAGCAGAGGGTACTCAAAGTTTGGGTTTCATGGACTAGTGCCAGTTT CACAAATTGTTA (195)	98%(191/195, e=5 ⁻⁹¹) Homo sapiens telomerase-associated protein 1 (TEP1), mRNA	3' UTR	Nucleus
hSC 4	GAGAGAAAGGGGATGTATCCCATGGGGGGCAGGGCATGA (39)	95%(37/39, e=8 ⁻⁰⁵) Homo sapiens glial fibrillary acidic protein (GFAP), transcript variant 1, mRNA	3' UTR	Cytoplasm
hSC 5	CACAGAAAATGA (12)	100% (12/12, e=28) Homo sapiens DEAD (Asp-Glu-Ala-Asp) box polypeptide 52 (DDX52), transcript variant X1, mRNA	3' UTR	Nucleus
hSC 6	ATGATGACTATGCAGGCTTTATCTTTGGCTACCAAGATAGCTCCAGCTTCTACGTGGTCTATGTGGAAGCAGACGGAGCAGACATATTG GCAAGCCACCCCATTCGAGCAGTTGCAGACCTGCATTACAGCTCAGCTGTGAAGTCTAA (147)	100% (12/12, e=28) Homo sapiens MACRO domain containing 2 (MACROD2), transcript variant X2, mRNA	coding	Nucleus
		100% (12/12, e=28) Homo sapiens zinc finger protein 528 (ZNF528), transcript variant X15, mRNA	5' UTR	Nucleus
		97% (147/151, e=1 ⁻⁶⁶) Homo sapiens thrombospondin 4 (THBS4), mRNA	coding	Endoplasmatic reticulum, sarcoplasmatic Reticulum
hSC 7	GGACAAGATGCCACTGCTTTTCTTAGCACTCTTCCCTCCCTAAACCATCCCGTAGTCTTCTACTATAGTCTCTCAGACAAGTGTCTCTAGATGGATGTGAACTCCTTAACTCATCAAGTAAGGTGGTACTCAAGCTATGCTGCCTCCTTACATCCTTTTTGGAAACAGAGCACGGTATAA (180)	98% (177/180, e=2 ⁻⁸⁵) Homo sapiens dysbindin (dystrobrevin binding protein 1) domain containing 2 (DBNDD2), transcript variant 1-9, mRNA	3' UTR	Cytoplasm
hSC 8	CTCTTTCTGACTACAACATCCCAGAAAGAGTCGACCCTGCACCTGGCTGCGCCTGAGGGGTGGCTGTTA (72)	99% (71/72, e=1 ⁻²⁸) Homo sapiens ubiquitin B (UBB), transcript variant 1-6, mRNA	Coding	Cytoplasm, nucleus
hSC 9	CGCGCCGCGCTCGACATTAAGTCTTCAATTTCAAGTCTAGCTTAA (45)	100% (30/30, e=7 ⁻⁰⁹) Homo sapiens kelch-like family member 42 (KLHL42), mRNA	3' UTR	Cytoplasm
hSC 10	GCCTTGATGGAGGAGGGAGGGCTTCAGGACGGGGCGTCAGAGGGAGCCCCCTCTGGGAGGGAACCAACCCCCACCCTCCCCCTCTGGGACCCCCCAGCATAGACGGCTTGGGGGAGTCCGGAGGCTCCCCGGCAGACACCCACCCCATCTTGTTCGCTTGA (162)	97% (159/164, e=3 ⁻⁷²) Homo sapiens TSC22 domain family, member 4 (TSC22D4), mRNA	3' UTR	Nucleus

hSC 11	TTGAGTCATCAAAAGTGCTTTTATTTGTAA (30)	97% (28/29, $e=8^{-04}$) Homo sapiens phosphatidylinositol-5-phosphate 4-kinase, type II, alpha (PIP4K2A), transcript variant X1, mRNA	3' UTR	Cellular membrane, nucleus, cytoplasm
hSC 12	CGAGACCAGCCATGGCCAACATGGTGA (27)	96% (26/27, $e=4^{-05}$) Homo sapiens nucleoporin 43kDa (NUP43), transcript variant 1-X1, mRNA	3' UTR	Nucleus
hSC 13	GGGGCCGGCAGGGGTTGGGGAAGAAGA GGGCTCAGGCCAGCAGGGGTGGAAGCC CCTGCCACTGCCACTACCCGCTCCAGAGCT TTAA (90)	96% (24/25, $e=7^{-04}$) Homo sapiens ATP synthase, H ⁺ transporting, mitochondrial Fo complex, subunit s (factor B) (ATP5S), transcript variant 1-2-X3-4, mRNA 100% (90/90, $e=8^{-41}$) Homo sapiens endothelin converting enzyme 1 (ECE1), transcript variant 12-3-4-X1, mRNA	3' UTR	Mitochondrion Cellular membrane
hSC 14	TTGATATTAAAACTAGTCTGTGTTCTTTG CAGTTTCTGTAAATTTATAAACAGGCACA AGGTTCAAGTTTAGATTTTAAGCACTTTTAT AACAAATGATAAGTGCCTTTTGGAGATGTAA CTTTTAGCAGTTTGTAACTGA (147)	100% (147/147, $e=3^{-72}$) Homo sapiens cell division cycle associated 7 (CDCA7), transcript variant 1-2, mRNA	3' UTR	Nucleus, cytoplasm
hSC 15	CTGGACAATGACAAGTACATCGCCCTGGATG AGTGGGCCGGCTGCTTCGGCATCAAGCAGA AGGATATCGACAAGGATCTTGTGATCTAA (90)	100% (90/90, $e=8^{-41}$) Homo sapiens secreted protein, acidic, cysteine-rich (osteonectin) (SPARC), mRNA	Coding	Extracellular matrix
hSC 16	AGTTGTAATATGATAGTGTGA (21)	100% (15/15, $e=1,4$) Homo sapiens PR domain containing 5 (PRDM5), transcript variant X1-2, mRNA	3' UTR	Nucleus
hSC 17	GGCGGGGAATCGCTTGA (18)	100% (18/18, $e=0,011$) Homo sapiens CGRP receptor component (CRCP), transcript variant 1-2-3-4, mRNA	3' UTR	Nucleus, cellular membrane
hSC 18	GAATGGCAACTGCTCTGCCTTTAGTCGCTG AGGAAAAATAAAGACAAATGCTGCGCCCTT (60)	96%(55/57, $e=8^{-19}$) Homo sapiens glial fibrillary acidic protein (GFAP), transcript variant 1, mRNA	3' UTR	Cytoplasm
hSC 19	AGTTTCGGTAGTTAAGTGAATTAAGGTC TAGAGTGA (38)	100% (38/38, $e=9e-14$) Homo sapiens SOGA family member 3 (SOGA3), mRNA	3' UTR	Cellular membrane
hSC 20	AGGAGTTCGCGCTGCCTACGAGGCTGCC GTGCTGCCACCTCCACCCCTGCGAGGTGG CGCTGCACTGA (71)	100% (38/38, $e=9e-14$) Homo sapiens KIAA0408, mRNA 100% (71/71, $e=2^{-30}$) Homo sapiens meteorin, glial cell differentiation regulator (METRN), mRNA	3' UTR Coding	- Secreted
hSC 21	CAGTTCCTCCCTCCCCACATTCCTGACAC TAGGTAAGACCCAATAA (47)	96%(45/47, $e=8^{-12}$) Homo sapiens myelin-associated oligodendrocyte basic protein (MOBP), transcript variant 3 and 1, non-coding RNA	3' UTR	Cytoplasm
hSC 22	CAGGTAGAGGAGGAGGTGGAGATGGGGTCA GGGAACATCTGGCAGAGGGAGTCCCAGTC TGTGTCTCCATCAGGCTTAA (80)	99% (68/69, $e=5^{-27}$) Homo sapiens TNFAIP3 interacting protein 2 (TNIP2), transcript variant 1, 2 and X1, mRNA	3' UTR	Cytoplasm, nucleus
hSC 23	TATTAATATATAGCCTCGATGATGAGAGAG TTACAAAGAACAATACTCCAGACACAAACC TCCAAATTTTTAGCAGAAAGCACTCTGCGT CGCTGAGCTGA (101)	Homo sapiens myelin basic protein (MBP), transcript variant 1, 2-4, 7 and X3, mRNA	3' UTR	Myelin membrane
hSC 24	GGGTGCCAATCGTCTTAA (18)	100% (13/13, $e=11$) Homo sapiens YTH domain containing 2, transcript variant X1, mRNA 100% (13/13, $e=11$) Homo sapiens transcription elongation regulator 1-like (TCERG1L), mRNA	Coding 3' UTR	Cytoplasm -
hSC 25	GGGTGCCAATCGTCTTAACTACTCAGGAGG GCTGA (35)	100% (13/13, $e=11$) Homo sapiens Alstrom syndrome 1 (ALMS1), mRNA 100% (16/16, $e=1.1$) Homo sapiens LYR motif containing 2 (LYRM2), transcript variant 1, non-coding RNA	Coding 3' UTR	Cytoplasm Mitochondrion
hSC 26	CAAATGTGGCAATTTTGGATCTATCAC CTGTCATCAACTGGCTTCTGCTTGTGCAT CCACACAACACCAGGACTTAAGACAAATG	100% (160/160, $e=2e-79$) Homo sapiens tumor protein, translationally-controlled 1 (TPT1), transcript variant 1-3, mRNA	3' UTR	Cytoplasm

hSC 27	GGACTGATGTCATCTTGAGCTCTTCATTTA TTTTGACTGTGATTTATTTGGAGTGGAGGC ATTGTTTTTAA (160) CTTTTTCAAAAAACATTAATTCACATGCA GTCTCTGA (38)	100% (35/35, e=6e-12) Homo sapiens phosphoprotein enriched in astrocytes 15 (PEA15), transcript variant X5-3, mRNA	3' UTR	Cytoplasm
hSC 28	AGAGTTCCTGA (11)	100% (11/11, e=112) Homo sapiens leukocyte specific transcript 1 (LST1), transcript variant X1-7, mRNA	5' UTR	Cellular membrane, golgi apparatus
		100% (11/11, e=112) Homo sapiens zinc finger protein 280C (ZNF280C), transcript variant X1, mRNA	coding	Nucleus
		100% (11/11, e=112) Homo sapiens Ras-related GTP binding B (RRAGB), transcript variant X1, mRNA	coding	Cytoplasm, lysosome
		100% (11/11, e=112) Homo sapiens Rho GTPase activating protein 6 (ARHGAP6), transcript variant X2-3, mRNA	coding	Cytoplasm
		100% (11/11, e=112) Homo sapiens MICAL-like 1 (MICALL1), transcript variant X1-3, mRNA	3' UTR	Membrane coat
hSC 29	TCCTCAAGGAGCAGAGCTCATCCAGCTTTC AGCCAGGGCCAGAGCTCCTAGAACTGAGC TGCCCTACCACAGCCTCCTGCCACCAGC TGGCCTCACCTCCTGAAGGCCCGGGTCA GACCTGCTCTCCTGGCGCAGTCCAGCT ATCTCCCCTGCTCCTCTGCTGGTGGTGGGC TAA (181)	99%(180/181, e=8e-89) Homo sapiens keratin 16 (KRT16), mRNA	Partly coding	Intermediate filament
hSC 30	GAGAGAGAGGAGAGAAGGATATTCCTGGAC TGACTGA (37)	100% (30/30, e= 5^-09) Homo sapiens ribosomal protein S6, mRNA	Coding	Cytoplasm, nucleus
hSC 31	AAATTCATAGGATAAGTCAATACCTTAA (28)	100% (28/28, e=5e-08) Homo sapiens reticulon 3, transcript variant 1-7, mRNA	3' UTR	Endoplasmatic reticulum, golgi apparatus
hSC 32	GGCACTAGTCCACAGAATTA (22)	100% (14/14, e=5.4) Homo sapiens general transcription factor IIIC, polypeptide 3, 102kDa (GTF3C3), transcript variant X1 and 1, mRNA	3' UTR	Nucleus
		100% (14/14, e=5.4) Homo sapiens topoisomerase (DNA) III alpha (TOP3A), transcript variant X1-2, mRNA	Coding (X1), 5' UTR (X2)	-
		100% (14/14, e=5.4) Homo sapiens CWF19-like 1, cell cycle control (S. pombe) (CWF19L1), mRNA	Coding	-
hSC 33	CCAGCACAGGTATTTTCAGGTGTGAAAGAAT CAGTAGGACCAAGCCACCGCTAGTGCTTGT GGAGATCACAGCCCCACCCCTTGCCCTCAG CAACATCCCATCTAAGCATTCCCACTGCAG GGAGGAGTGGTACTTAAGCTCCCCTGCCTT AACCTGGGACCAACCTGA (169)	100% (169/169, e=2^-84) Homo sapiens transcription factor binding to IGHM enhancer 3 (TFE3), transcript variant1, 2 and X1, mRNA	3' UTR	Nucleus
hSC 34	AGAGGAACTAGTCTCGAG (18)	100% (13/13, e=11) Homo sapiens programmed cell death 6 interacting protein (PDCD6IP), transcript variant 1-2, mRNA	3' UTR	Cytoplasm
		100% (13/1, e=11) Homo sapiens nitrilase 1 (NIT1), transcript variant 2, mRNA	3' UTR	Cytoplasm, mitochondrion
hSC 35	CCAGCACAGGTATTTTCAGGTGTGAAAGAAT CAGTAGGACCAAGCCACCGCTAGTGCTTGT GGAGATCACAGCCCCACCCCTTGCCCTCAG CAACATCCCATCTAAGCATTCCCACTGCAG GGAGGAGTGGTACTTAAGCTCCCCTGCCTTA ACCTGGGACCAACCTGACCTAA (174)	100% (174/174, e=4^-87) Homo sapiens transcription factor binding to IGHM enhancer 3 (TFE3), transcript variant 1,2 and X1, mRNA	3' UTR	Nucleus

hSC 36	CAGAACTTAA (10)	100% (10/10, e=443) Homo sapiens uncharacterized LOC285556 (LOC285556), transcript variant X1-3, mRNA	3' UTR	-
		100% (10/10, e=443) Homo sapiens KAT8 regulatory NSL complex subunit 1 (KANSL1), transcript variant X1-4, mRNA	3' UTR	Nucleus
		100% (10/10, e=443) Homo sapiens Rho guanine nucleotide exchange factor (GEF) 10 (ARHGEF10), transcript variant X1-8, mRNA	coding	Cytoplasm
		100% (10/10, e=443) Homo sapiens serologically defined colon cancer antigen 8 (SDCCAG8), transcript variant X4, mRNA	Coding (X8 = 5' UTR)	Cytoplasm
		100% (10/10, e=443) Homo sapiens serologically defined colon cancer antigen 8 (SDCCAG8), transcript variant X1-6 and X8-10, mRNA	3' UTR	Cytoplasm, nucleus
hSC 37	GAGAGAGAGAGAGAGAGAGAACTAGTCTCGA (31)	100% (22/22, e=2e-04) Homo sapiens DEAD (Asp-Glu-Ala-Asp) box helicase 3, Y-linked (DDX3Y), transcript variant X3, mRNA	3' UTR	Cytoplasm, cellular membrane
		100% (22/22, e=2e-04) Homo sapiens chloride intracellular channel 6 (CLIC6), transcript variant X1, mRNA	3' UTR	Nucleus
hSC 38	GACGTCAGATCGCCTTCCCCGTAA (25)	100% (22/22, e=2e-04) Homo sapiens MRE11 meiotic recombination 11 homolog A (S. cerevisiae) (MRE11A), transcript variant 1-2, mRNA	3' UTR	Nucleus
		100% (14/14, e=8,1) Homo sapiens ectonucleoside triphosphate diphosphohydrolase 6 (putative) (ENTPD6), transcript variant X11-12, mRNA	Coding	Golgi apparatus
		100% (14/14, e=8.1) Homo sapiens ADAM metalloproteinase with thrombospondin type 1 motif, 10 (ADAMTS10), transcript variant X4-5, mRNA	Coding, 5'UTR	Extracellular matrix
		100% (14/14, e=8.1) Homo sapiens Rho GTPase activating protein 44 (ARHGAP44), transcript variant X5, mRNA	Coding	Synapse
hSC 39	GTTTGAACCTCTTCTTTGCCAGGTGTGAGGACTTCTGCATCTTACAGTCAGCACAGAACACACTGAGACTTGAATCAAGTCAGCAACAGAGCAAATAAAGGTTAGATAA (109)	100% (14/14, e=8.1) Homo sapiens dual oxidase maturation factor 1 (DUOXA1), transcript variant X1-5, X7-9 and X12-17, mRNA	5' UTR	Cellular membrane
		100% (109/109, e=3e-51) Homo sapiens calpastatin (CAST), transcript variant X1-20, 2, 6, 11, 13 and 14, mRNA	3' UTR	Cytoplasm, cellular membrane

3' UTR=3' untranslated region, 5' UTR=5' untranslated region, hSC=human spinal cord

Auteursrechtelijke overeenkomst

Ik/wij verlenen het wereldwijde auteursrecht voor de ingediende eindverhandeling:

Development and serological analysis of a human spinal cord cDNA phage display library

Richting: **master in de biomedische wetenschappen-klinische moleculaire wetenschappen**

Jaar: **2014**

in alle mogelijke mediaformaten, - bestaande en in de toekomst te ontwikkelen - , aan de Universiteit Hasselt.

Niet tegenstaand deze toekenning van het auteursrecht aan de Universiteit Hasselt behoud ik als auteur het recht om de eindverhandeling, - in zijn geheel of gedeeltelijk -, vrij te reproduceren, (her)publiceren of distribueren zonder de toelating te moeten verkrijgen van de Universiteit Hasselt.

Ik bevestig dat de eindverhandeling mijn origineel werk is, en dat ik het recht heb om de rechten te verlenen die in deze overeenkomst worden beschreven. Ik verklaar tevens dat de eindverhandeling, naar mijn weten, het auteursrecht van anderen niet overtreedt.

Ik verklaar tevens dat ik voor het materiaal in de eindverhandeling dat beschermd wordt door het auteursrecht, de nodige toelatingen heb verkregen zodat ik deze ook aan de Universiteit Hasselt kan overdragen en dat dit duidelijk in de tekst en inhoud van de eindverhandeling werd genotificeerd.

Universiteit Hasselt zal mij als auteur(s) van de eindverhandeling identificeren en zal geen wijzigingen aanbrengen aan de eindverhandeling, uitgezonderd deze toegelaten door deze overeenkomst.

Voor akkoord,

Drieskens, Sarah

Datum: **10/06/2014**